PERGAMON

Quaternary Science Reviews 18 (1999) 1021–1038

QSR

Holocene climate variability in Europe: Evidence from $\delta^{18}O$, textural and extension-rate variations in three speleothems

Frank McDermott[a,*], Silvia Frisia[b], Yiming Huang[c,d], Antonio Longinelli[e], Baruch Spiro[f], Tim H.E. Heaton,[f] Chris J. Hawkesworth[c], Andrea Borsato[b], Eddy Keppens[g], Ian J. Fairchild[d], Klaas van der Borg[h], Sophie Verheyden[g], Enrico Selmo[e]

[a]*Department of Geology, University College Dublin, Belfield, Dublin 4, Ireland*
[b]*Museo Tridentino di Scienze Naturali, via Calepina 14, Trento, Italy*
[c]*Department of Earth Sciences, The Open University, Walton Hall, Milton Keynes, MK7 6AA, UK*
[d]*Department of Earth Sciences, Keele University, Staffordshire, ST5 5BG, UK*
[e]*Dipartimento Scienze della Terra, Via E. Weiss 6, University of Trieste, Trieste 34100, Italy*
[f]*NERC Isotope Geosciences Laboratory, Keyworth, Nottingham, UK*
[g]*Department of Geochronology, Vrije Universiteit Brussel, Pleinlaan 2, B-1050 Brussel, Belgium*
[h]*Department of sub-Atomic Physics, Van de Graff laboratory, University of Utrecht, Princetonplein 5, Utrecht, Netherlands*

Abstract

Time-series O isotope profiles for three U–Th dated stalagmites have revealed that for much of the Holocene, a site on the Atlantic seaboard (SW Ireland) exhibits first-order $\delta^{18}O$ trends that are almost exactly out of phase with coupled $\delta^{18}O$ curves from two southern European sites (SE France and NW Italy). In the Irish stalagmite (CC3 from Crag Cave, SW Ireland), low $\delta^{18}O$ at 10,000 cal yr BP reflects cool conditions. By the early to mid-Holocene (9000–6000 cal yr BP) $\delta^{18}O$ had increased, reflecting the onset of warmer conditions on the Atlantic seaboard. This shift to higher $\delta^{18}O$ was accompanied by a marked increase in the stalagmite extension rate, reinforcing our interpretation that this was a period of relative warmth. Except for an episode of increased extension rate about 5500 yr ago, $\delta^{18}O$ in the Crag stalagmite exhibits a gradual decrease, accompanied by declining extension rates between 7800 and 3500 cal yr BP, interpreted as a cooling trend. There is evidence for increases in both $\delta^{18}O$ and stalagmite extension rate in the period from 3500 cal yr BP to the present day suggesting a return to warmer conditions on the Atlantic seaboard. In the stalagmite from NW Italy (ER76, Grotta di Ernesto, Trentino province) the early-Holocene (c. 9200-7800 cal yr BP) is characterised by high $\delta^{18}O$, probably indicative of warm and/or dry conditions. Exceptionally low $\delta^{18}O$ from 7800 to 6900 cal yr BP at this site reflects a well-defined wet phase (Cerin wet phase). In the last three millennia, this stalagmite exhibits a shift to lower $\delta^{18}O$, interpreted as some combination of cooler and/or wetter conditions. Unlike the Irish stalagmite, the Italian sample does not show a correlation between $\delta^{18}O$ and extension rate. Instead, its extension rate correlates roughly with $\delta^{13}C$, presumably reflecting a climate-driven vegetation change. In the early Holocene, $\delta^{18}O$ in the French stalagmite (CL26, Grotte de Clamouse, Herault province, SE France) was low relative to its Holocene average. For much of the period since c. 3500 cal yr BP this stalagmite exhibits higher $\delta^{18}O$ than in the early Holocene, suggesting warmer conditions. Like the Irish stalagmite, the French sample exhibits a well-defined correlation between $\delta^{18}O$ and extension rate. Had drip-water availability been the dominant control on $\delta^{18}O$ at this semi-arid site then higher $\delta^{18}O$ would have been accompanied by lower, not higher extension rates. This suggests strongly that temperature rather than rainfall amount was the dominant control at this site. While conclusions regarding the patterns of climate variability on a continent scale must remain tentative because of the limited number of stalagmites studied we argue that early Holocene warm conditions on the Atlantic seaboard (Irish site) coincided with relatively cool conditions at the Clamouse site. By c. 3500 yr ago the pattern appears to have been reversed. © 1999 Elsevier Science Ltd. All rights reserved.

1. Introduction

By comparison with the rapid, high amplitude fluctuations that characterised the last glaciation (Atkinson

* Corresponding author. Tel.: 00 353 1 706 2328; fax: 00 353 1 283 7733

PII: S 0 2 7 7 - 3 7 9 1 (9 8) 0 0 1 0 7 - 3

et al., 1987; Taylor *et al.*, 1993; Dansgaard *et al.*, 1993), climate change in the Holocene was relatively subtle. Nonetheless, several types of proxy data (pollen and coleoptera, peat macrofossils, glacier and tree lines, lake levels, tree rings, lacustrine carbonates and ice cores) indicate detectable changes in temperature and/or moisture balance (e.g. Huntley and Prentice, 1993; Guiot *et al.*, 1993; Barber *et al.*, 1994; Chambers *et al.*, 1997; Nesje and Kvamme, 1991; O'Brien *et al.*, 1995; Magny, 1995). Progress in understanding the nature and causes of Holocene climate variability on a global scale has been hampered by (i) difficulties in correlating between relatively weak, short lived and often poorly dated proxy signals (Alley *et al.*, 1997) and (ii) increasing evidence for diachroneity or even decoupling on regional scales, in for example N. America (Wright, 1992; Yu *et al.*, 1997), and Europe (Guiot *et al.*, 1993; Lamb *et al.*, 1995; Harrison *et al.*, 1996).

In this study we focus on three sites in western Europe, a region characterised in the present day by several climate zones. Several aspects of this region's Holocene climate which are essential to test the validity of General Circulation Models (GCMs; e.g. COHMAP Members, 1988; Kutzbach and Guetter, 1986; Kutzbach *et al.*, 1993; Hall and Valdes, 1997) remain poorly understood. Some addressed in this study include; (i) the timing, duration and geographical extent of the so-called 'Mid-Holocene climatic optimum', (ii) the relationship between Holocene climatic conditions on the Atlantic seaboard and the N. Mediterranean region (e.g. Guiot *et al.*, 1993; Cheddadi *et al.*, 1997) and (iii) the extent to which the present-day zonal pattern of atmospheric circulation over W. Europe was stable through the Holocene.

Many studies of continental palaeoclimate are based on oxygen isotopes, because in circumstances where the $\delta^{18}O$ of water from which authigenic carbonates (e.g. speleothems) were precipitated is known or can be inferred independently, a record of relative or even absolute temperature changes can be reconstructed (e.g. Schwarcz, 1986; Goede *et al.*, 1986; Gascoyne, 1992; Talma and Vogel, 1992; Lauritzen, 1995). Typically however, other factors such as changing moisture sources, air mass history, rainfall seasonality and amount, and moisture recycling can also influence $\delta^{18}O$ in continental precipitation (Grootes, 1993). In the case of cave carbonates additional complications arise, especially in arid and semi-arid regions because the $\delta^{18}O$ of precipitation may be modified by evaporation processes at or near the surface (e.g. Bar-Matthews *et al.*, 1996).

At present there is still a paucity in Europe of well-dated oxygen isotopic records for Holocene authigenic carbonates. Therefore, in this study we present new oxygen and accompanying carbon isotope time-series data for three U–Th dated Holocene stalagmites from caves in W. Europe (SW Ireland, SE France and NE Italy, Fig. 1). The Irish site was chosen because of its proximity to the North Atlantic ocean which has a central role in many models for late and post-glacial climate change on sub-Milankovitch timescales (e.g. Ruddiman and McIntyre, 1981; Broecker, 1991). The French site was selected for its location on the Mediterranean seaboard, and because the dry climate of the region contrasts sharply with that of Ireland. The Italian site was chosen for its location at the southern margin of the Alps and its sub-continental climatic conditions. Here we focus on the oxygen isotope data and its palaeoclimatic interpretation. The accompanying carbon isotope data will be discussed in detail elsewhere (McDermott *et al.*, in prep.; Heaton *et al.*, in prep.). Data from a fourth site (Pére Noël, Belgium) are more complex because there is evidence for variably evaporative and rapid degassing conditions, and these will be presented elsewhere (Verheyden *et al.*, in prep.).

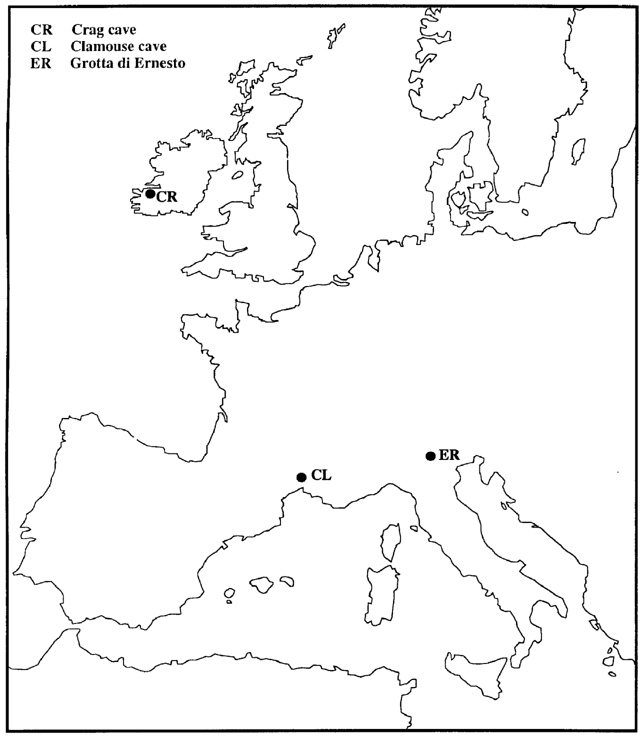

Fig. 1. Map of W. Europe showing the location of the three cave sites discussed in this study. CR = Crag Cave, SW Ireland; CL = Grotte de Clamouse, SE France; ER = Grotta di Ernesto, Italy.

2. Site selection and descriptions

Crag cave is developed in Lower Carboniferous limestones, some 20 km from the Atlantic coast of SW Ireland (Fig. 1). The cave entrance is approximately 60 m a.s.l., and is located 35 km south of the Southern Irish End-Moraine (McCabe, 1987). The studies described here were carried out in the cave interior (beyond the present show-cave) of this relatively shallow cave (c. 20 m deep) where the relative humidity is high (98–99%). Drip water and air temperature measurements indicate that the temperature was stable at 10.4°C during the two-year period of this study. The present-day climate of SW Ireland is maritime, mild and wet, dominated by westerly winds and moderated by the N. Atlantic Gulf Stream. Data from four meteorological stations in the region indicate mean annual air temperatures (m.a.a.t.) in the range 9.5–11.5°C depending on elevation, and inter-annual m.a.a.t. variations of ± 0.5°C are typical. The mean annual precipitation at two weather stations within 15 km of the cave, at Glountaine (elevation 241 m a.s.l.) and Reenagown (187 m a.s.l.) are 1465 ± 284 and 1485 ± 292 mm, respectively (45 yr averages $\pm 2\sigma$ mean).

Grotte de Clamouse (latitude 43°42′33″N; longitude 3°36′50″E) is located 30 km west of Montpellier (Herault province, southern France) at 75 m a.s.l. The cave is developed in upper Jurassic (Tithonian) dolomites which are partially dedolomitised. The present-day climate in the area is sub-humid Mediterranean, characterised by strong seasonal contrasts which increase from the coast (Montpellier) to the foothills (Gignac, Aniane). Mean annual precipitation for the period 1965–1995 is 791 mm at Aniane and 742 mm at Gignac. The most striking feature in the climate of the Herault province is the summer dryness, which coupled with the high evapotranspiration results in a water deficit during June, July and August. The mean annual temperature of the cave air and water is 14.5 ± 0.1°C (Borsato *et al*., in prep.). The stalagmite removed for detailed study (CL26) was from 'Le Balcon', a chamber in the uppermost level of the cave, approximately 80 m beneath the surface.

Grotta di Ernesto is located 1165 m a.s.l. (latitude 45°58′37″, longitude 11°39′28″) on the northern slope of Valsugana valley (Trento province) in NE Italy. The cave consists of a single downdipping gallery developed along a NW trending sub-vertical fault in pervasively dolomitised oolitic limestone of the lower Jurassic which is overlain by massive, red limestones and marly limestones. Mean annual precipitation fluctuates between 1000 and 1500 mm, and exhibits a bimodal distribution with maxima in May–June and in October–November (Borsato *et al*., 1996). Snowfall occurs mostly from December to March, and snowmelt occurs between mid-March and early April. The mean annual temperature of the cave air is 6.6 ± 0.1°C and the relative humidity is c. 98.5–99.5%. The stalagmite removed for study (ER76) was from the main chamber (Sala Grande) of this relatively shallow (c. 22 m deep), small (72 m long) cave.

3. Sample selection and analytical procedures

Reconnaissance U–Th dates were obtained for small cores drilled from the bases of several stalagmites in Crag cave (SW Ireland), Grotte de Clamouse (SE France) and Grotta di Ernesto (NE Italy), (Fig. 1). For conservation reasons, only one Holocene stalagmite was subsequently removed from each cave for detailed petrographic, dating and geochemical studies. $\delta^{18}O$ and $\delta^{13}C$ studies were also completed on a variety of modern calcite precipitates and waters from each site.

High-precision U–Th dating (7–11 dates per stalagmite) was carried out at regular intervals along the extension axis of each stalagmite (Table 1). Unlike radiocarbon dating, this technique yields ages directly in calendar years. Calcite samples for U–Th dating (0.2–2 g) were dissolved and equilibrated with a mixed ^{229}Th–^{236}U spike. U and Th were separated on columns containing 2 mls of anion exchange resin (1 × 8 AG, 200–400 mesh Biorad). The total procedural blanks were negligible (c.15 pg of ^{232}Th and ^{238}U). Th and U fractions were loaded onto outgassed graphite-coated Re-filaments, and the isotope ratios were measured using a Finnigan MAT 262 RPQ-2 mass spectrometer. The typical abundance sensitivity was 5×10^{-8} at mass 237 (1 amu below the major ^{238}U peak), hence tail contributions at masses 230 and 234 from the large ^{232}Th and ^{238}U peaks were negligible. ^{230}Th/^{229}Th, ^{232}Th/^{229}Th, ^{234}U/^{236}U and ^{235}U/^{236}U atomic ratios were measured in peak-switching ion-counting mode. Errors based on the counting statistics were $< 0.1‰$ for all ratios except for ^{230}Th/^{229}Th, where the small number of ^{230}Th ions result in a relative error of typically 0.4–1.0% (2σ) depending on the U content and age of the sample.

Samples from the Grotta di Ernesto stalagmite (ER76) had exceptionally low ^{230}Th contents (< 0.07 pg g^{-1}) because of their low U contents and relatively young ages (Table 1). In these samples the age uncertainties were significantly higher than 1%, and are estimated to be up to $\pm 3\%$ at the 2σ level for some samples (Table 1).

Samples for stable isotope measurements were drilled from 1 mm pits at regular intervals (typically 2–2.5 mm) along the central growth axis of each speleothem. Stable isotope ratios were measured both at the NERC Isotope Geosciences Laboratory (NIGL, UK) and at the University of Trieste, Italy. The calcite samples were reacted with 100% phosphoric acid, and the resultant CO_2 was cryogenically purified prior to mass spectrometric analysis. Water $^{18}O/^{16}O$ ratios were analysed following equilibration with CO_2. By comparison with laboratory marble and water standards calibrated against NBS and IAEA reference materials, the sample $^{18}O/^{16}O$ ratios are reported as $\delta^{18}O$ values in per mil versus VPDB (for carbonates) and versus VSMOW (for waters). Analytical precisions were $< 0.2‰$ (2σ), and where the same calcite or water samples were analysed by both laboratories, the results agreed within these limits. Ages were assigned to the stable isotope samples using a simple linear interpolation between the positions selected for U–Th dating.

Table 1. Mass-spectrometric U-Th age data for speleothems from Crag Cave (Ireland), Grotte de Clamouse (France) and Grotta di Ernesto (Italy). Decay constants used to calculate activity ratios from measured atomic ratios are as follows; $\lambda^{238}U = 1.551E-10$, $\lambda^{234}U = 2.835E-6$, $\lambda^{230}Th = 9.915E-6$, $\lambda\ ^{232}Th = 4.948E-11$. Age uncertainties are reported at the 1σ level.

Sample No	Distance from tip (mm)	^{238}U (ppm)	(^{234}U/^{238}U)	^{230}Th (pg/g)	(^{230}Th/^{232}Th)	(^{230}Th/^{234}U)	**Age (kyr)**
Crag Cave (Ireland)							
CC3 20	20	4.831	0.956	0.815	19	0.0108	**1.18 ± 0.02**
CC3 20R	20	4.805	0.950	0.661	20	0.0089	**0.97 ± 0.02**
CC3 34	34	4.332	0.949	0.863	122	0.0129	**1.41 ± 0.01**
CC3 55	55	4.020	0.952	1.456	140	0.0234	**2.57 ± 0.02**
CC3 95	95	7.424	0.959	5.444	1307	0.0473	**5.27 ± 0.03**
CC3 100	100	7.057	1.002	5.657	554	0.0494	**5.51 ± 0.03**
CC3 146	146	7.199	0.954	5.944	535	0.0531	**5.94 ± 0.03**
CC3 250	250	8.427	0.955	9.599	2259	0.0732	**8.27 ± 0.05**
CC3 302	302	4.741	0.981	5.958	508	0.0786	**8.90 ± 0.03**
CC3 400	400	10.28	0.964	13.110	8920	0.0811	**9.21 ± 0.04**
CC3 450	450	4.026	0.986	5.466	2272	0.0845	**9.60 ± 0.07**
CC3 465	465	1.954	0.948	3.211	4420	0.1063	**12.24 ± 0.18**
Grotta di Ernesto (Italy)							
ER76-2B	62	0.041	2.111	0.0425	48	0.0302	**3.32 ± 0.02**
ER76-3B	102	0.042	2.089	0.0517	53	0.0366	**4.04 ± 0.04**
ER76-4B	151	0.041	2.037	0.0629	60	0.0468	**5.19 ± 0.11**
ER76-8b	313	0.036	1.714	0.0692	22	0.0692	**7.77 ± 0.09**
ER76-8a	323	0.026	1.881	0.0643	30	0.0818	**9.22 ± 0.13**
ER76B	368	0.019	1.743	0.0432	27	0.0815	**9.20 ± 0.15**
Grotto de Clamouse (France)							
CL26-1	6	0.095	4.349	0.017	50	0.0026	**0.282 ± 0.007**
CL26.2	68	4.746	4.362	3.607	24620	0.0107	**1.167 ± 0.003**
CL26-6	138.5	0.168	4.322	0.229	781	0.0194	**2.120 ± 0.011**
CL26-3	208.5	0.144	4.309	0.251	1794	0.0254	**2.788 ± 0.017**
CL26-7	277.5	0.118	4.231	0.286	1804	0.0351	**3.869 ± 0.031**
CL26.4	345	0.095	4.192	0.326	1897	0.0502	**5.568 ± 0.025**
CL26.9	378	0.063	4.228	0.277	1426	0.0639	**7.134 ± 0.031**
CL26.8	410	0.067	4.277	0.391	832	0.0823	**9.242 ± 0.042**
CL26-8R	410	0.067	4.346	0.394	878	0.0838	**9.423 ± 0.048**
CL26-5	476	0.099	4.040	0.641	775	0.0984	**11.127 ± 0.044**

Petrographic observations were carried out using conventional optical microscopy, SEM and transmission electron microscopy (TEM) on parts of each speleothem which were characterised by different crystal forms (Frisia, 1996; Frisia *et al*., unpublished data). TEM techniques allowed us to make qualitative inferences about the mechanisms and rates of crystal growth, which influence the morphology and reflect compositional variations of carbonates (Wenk *et al*., 1983; Frisia and Wenk, 1994).

4. Results

4.1. Petrography

Detailed petrographic observations of the analysed calcite are important for several reasons. First, by analogy with the textures of recently precipitated calcite we have been able to identify systematic textural variations that relate to drip-water availability (Frisia *et al*., in prep.). Second, detailed petrographic studies are essential to recognise and to quantify diagenetic phenomena (Ward and Reeder, 1993; Frisia and Wenk, 1994). Third, some studies (e.g. Paquette and Reeder; 1990; Dickson 1991, 1997; Paquette *et al*., 1993; Reeder, 1996) have challenged the assumption that 'equilibrium' isotope fractionation factors or partition coefficients can be applied without explicitly considering possible crystallographic controls.

All of the stalagmites studied here are composed of crystallites (Kendall and Broughton, 1978), the growth mechanism of which determines the habit of the larger polycrystals that are observed by optical microscopy. We use the term 'texture' to describe the general habit of the polycrystals and have used textural changes with time to construct textural logs. Each texture can be related to fluctuations in the physico-chemical parameters of the precipitating medium by applying the theoretical concepts of crystal nucleation and growth (Sunagawa, 1984). Nucleation and growth theory requires that the precipitation of calcite from solution requires a deviation from equilibrium in the form of supersaturation (Sunagawa, 1984). With increasing degrees of supersaturation, crystals are expected to pass from polyhedra with flat faces to polyhedra with stepped and kinked faces, to dendrites and eventually spherulites (Sunagawa, 1984; Jones and Kahle, 1993). These variations of crystal habits are mimicked by the textural changes that we have observed in the studied stalagmites (Fig. 2). The inference that they developed in conditions of increasing textural disequilibrium is confirmed by TEM observations of a trend from weakly defective crystallites to highly defective crystallites with increasing supersaturation of the precipitating waters (Frisia, S., unpublished data). Disturbances from

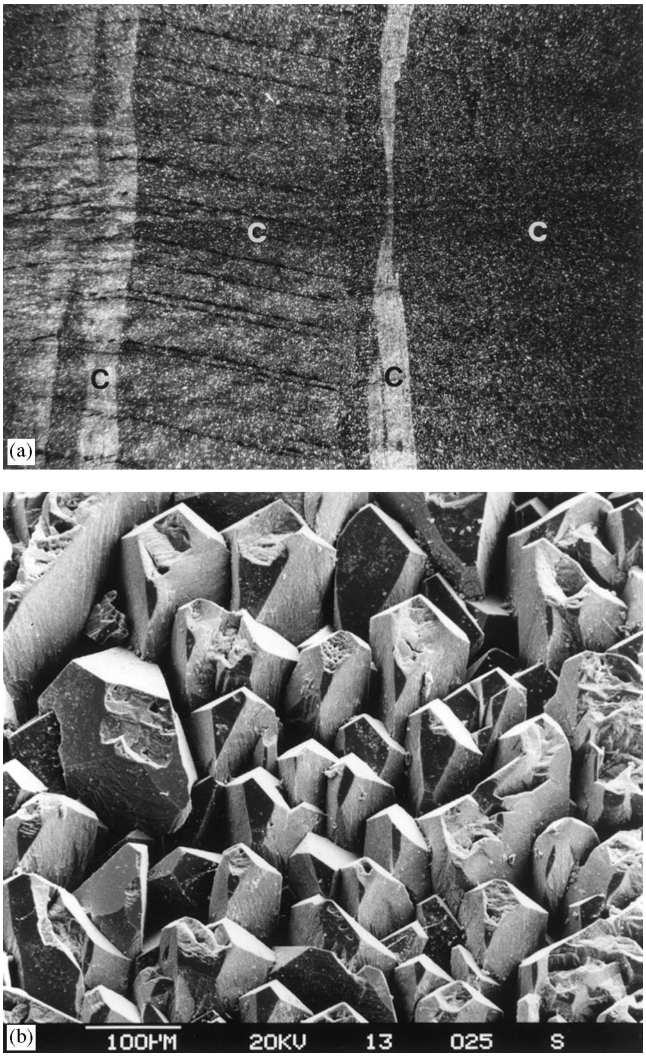

Fig. 2. Figures to illustrate typical textures described in the text. (a) Typical ancient columnar calcite preserved in the Crag stalagmite (CC3). These columnar (C) composite crystals exhibit straight boundaries, well developed cleavage planes and uniform extinction. The base of the picture is 10 mm across. Crossed polars. (b) SEM photomicrograph illustrating the morphology of present-day columnar calcite at Crag cave. Note that the tips of the crystals exhibit well-developed flat faces.

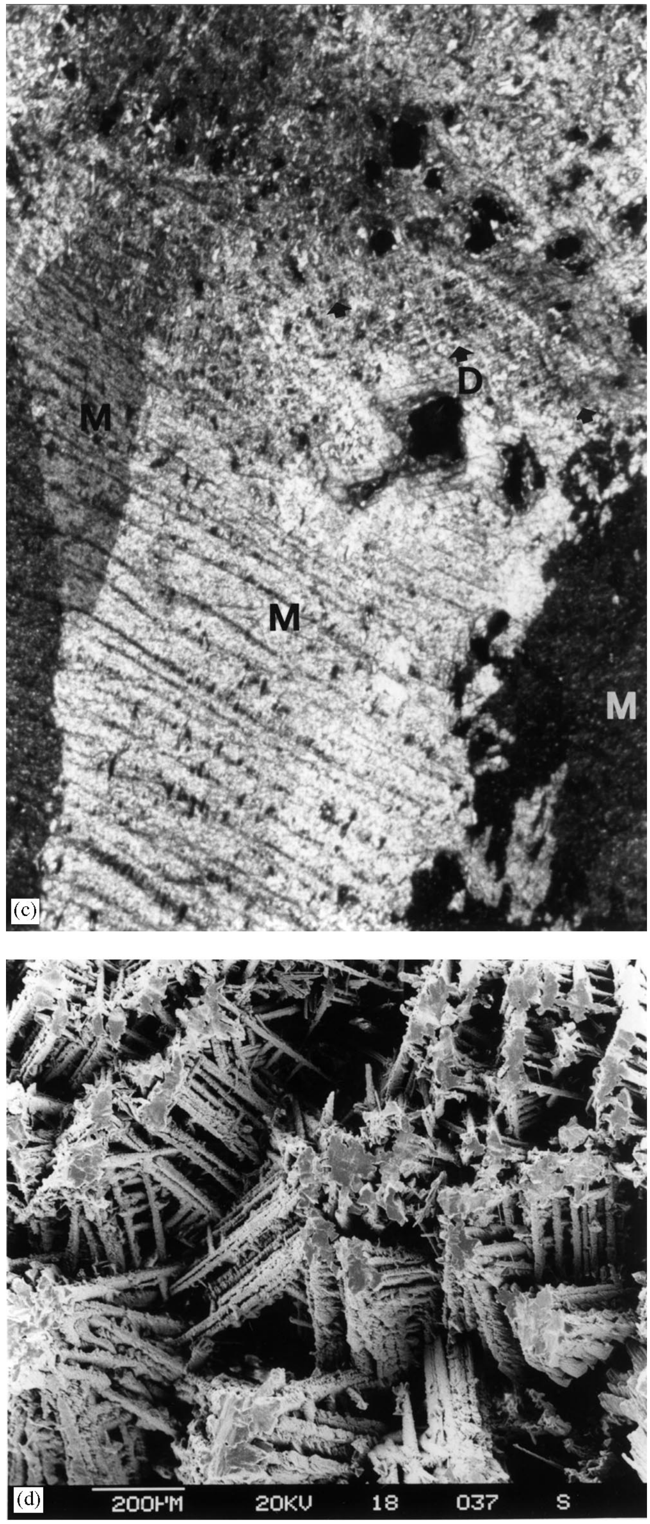

Fig. 2. (c) Typical ancient microcrystalline (M) and dendrite-like (arrows, D) calcite textures in the Grotta di Ernesto stalagmite (ER76). Cleavage planes are straight, regularly spaced and can be marked by triangular-shaped voids. (d) SEM micrograph of typical ancient dendrite-like texture in Crag cave stalagmite. Note the scaffold-like arrangement of the rods. Each rod is composed of rhombohedral crystallites.

equilibrium conditions may also be caused by the presence of impurities such as Mg, Ca clays and organic acids (Boistelle, 1982), although trace element data indicate that these effects were probably unimportant in the samples studied.

The identified textures are listed below in order from the lowest to the highest degree of textural disequilibrium, i.e. from the lowest deviation from saturation and/or the lowest content of impurities for the precipitating solution to the highest. The observed sequence is; (i) columnar calcite, (ii) microcrystalline calcite and (iii) dendrite-like calcite (Fig. 2). In addition two other forms have been recognised, namely equant calcite and acicular columnar calcite, both of which occur as neomorphic calcite after aragonite. Each form is described in more detail below (Fig. 2).

(i) Columnar calcite (Fig. 2a) consists of slightly to highly elongated, composite crystals (Kendall and Broughton, 1978) with straight to irregular intercrystalline boundaries, *c*-axes perpendicular to the substrate, elongation perpendicular to the substrate and uniform extinction. Two types of columnar calcite can be identified on the basis on crystal elongation and the crystal boundaries:

(a) Squat columnar, with a length to width ratio lower than 4 : 1, commonly 2 : 1. This form is characterised by few dislocations and few sub-grain boundaries, indicative of growth in near equilibrium conditions.
(b) Elongate columnar calcite, with a length to width ratio ranging from 4 : 1 up to 6 : 1. This exhibits more rugged crystal boundaries than the squat columnar type due to slight mismatch of crystallites.

(ii) Microcrystalline calcite (Fig. 2c) is typical of laminated stalagmites (e.g. parts of the Grotta di Ernesto stalagmite). The laminae consist of alternating layers of micron-sized calcite crystallites and layers consisting of organic matter, clay particles and sub-micron pores (Borsato *et al*., 1996; Frisia, 1996; Borsato *et al*., in prep.). The carbonate laminae consists of equant, planar-s to nonplanar (Sibley and Gregg, 1987) crystallites, up to 5 μm long. Each crystallite is characterised by a high density of defects, lamellae, twins and dislocations. Crystallites are arranged in domains with uniform extinction because they tend to exhibit a preferred orientation (Frisia, 1996). The high density of defects probably indicates that they grew in high supersaturation conditions.

(iii) Dendrite-like texture consists of aggregates of branching polycrystals (Fig. 2d). The composing crystallites are characterised by high dislocation density, and a great variety of sizes, ranging from 5 μm to less than 1 μm. Their sub-micron size and the lack of a distinct preferred orientation yields ringed diffraction patterns. Poor size distribution, high defect density and poor organisation indicate that dendrite texture develops in conditions of higher supersaturation (drier conditions) compared with those accompanying the formation of microcrystalline texture. In the Crag stalagmite (CC3) dendrite-like textures are frequently accompanied by a decrease in speleothem diameter suggesting that decreased water influx (drier conditions) were responsible for the development of these textures at this site (McDermott *et al*., in prep.). At Grotta di Ernesto (the other site where dendrite-like textures are observed) its development is often accompanied by coupled $\delta^{18}O$ and $\delta^{13}C$ shifts, suggesting that it result from drip-water evaporation within the cave. This in turn may reflect relatively dry conditions (Frisia *et al*., in prep.)

Equant calcite and acicular columnar calcite are typical of the stalagmites from Grotte de Clamouse. Equant calcite consists of polyhedral polycrystals with common rhombohedral form, whereas acicular calcite consists of crystals with a length-to-width ratio which can exceed 20 : 1. Both show aragonite micro-inclusions (Frisia, 1996). The results of the textural studies are presented as textural logs (coded 1–5) in Fig. 4, alongside the time-series stable isotope profiles to aid the interpretation of the latter.

4.2. U–Th dating

U–Th dating (Table 1) for the Crag stalagmite (CC3) indicates that deposition commenced prior to 12,236 ± 180 yr ago and continued until the present-day (actively growing when collected). This corresponds to a mean annual extension rate of 38 mm ka^{-1} (Fig. 3), although considerable extension-rate variations occurred through time (see below). Data for the Clamouse stalagmite (CL26) indicates that growth commenced at 11,127 ± 44 yr ago, and the U–Th date of 282 ± 7 yr obtained for a c. 2g sample centred on a point 6 mm from the top of the stalagmite is consistent with the observation that this stalagmite was also active when collected (mean extension-rate of 43 mm ka^{-1}). Dating of the upper part of the Grotta di Ernesto stalagmite (ER76) was more difficult due to low U contents (typically 0.03–0.05 ppm, Table 1). We were unable to obtain reliable dates for material above 62 mm from the base of the speleothem, because the ^{230}Th ion-beams obtained were too small and unstable to yield reliable $^{230}Th/^{229}Th$ ratios. A series of ages were obtained ranging from 9195 ± 140 yr at the base, to 3324 ± 22 yr for a sample 62 mm from the top of the stalagmite (mean extension-rate of 40 mm ka^{-1}). Unlike the other two stalagmites, distinct growth laminae are visible over several intervals in this stalagmite. Layer counting over two U–Th dated

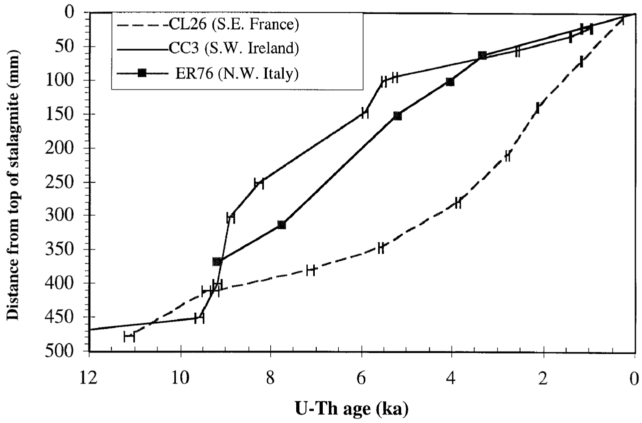

Fig. 3. Positions of samples taken for U–Th age measurements (distance in mm along the extension axis measured from the top of each of the three stalagmites) plotted against U–Th age. Ages assigned to the stable isotope curves and textural logs have been interpolated linearly between the dated points. U–Th data are given in Table 1.

intervals has demonstrated that these laminae are annual (Borsato *et al.*, in prep.), confirming a report that speleothems can preserve annual banding (Baker *et al.*, 1993). Using the available U–Th ages, growth laminae and the constraint that the upper surface of the stalagmite has a zero age (collected from an active drip-site and therefore actively growing when collected), a chronology was assigned to the upper 62 mm of the stalagmite (Fig. 3). None of the stalagmites studied here have obvious depositional hiatuses. With the exception of some short intervals of the Clamouse stalagmite (CL26) in which relict aragonite remains (Fig. 4c), all of the samples analysed for stable isotopes were calcite.

4.3. Time-series stable isotope data

This paper focuses on the oxygen isotope record, but the carbon isotope and petrographic data are discussed whenever these can contribute to the interpretation of the oxygen data. In Fig. 4a–c, the time-series oxygen, carbon and textural profiles are presented for each stalagmite in turn. $\delta^{18}O$ varies from -4.29 to $-1.95‰$ (PDB) in the Crag stalagmite (Fig. 4a) with the highest values occurring in the early Holocene. $\delta^{18}O$ decreases in the period c.7600 to 3500 yr before present, followed by an irregular trend to higher $\delta^{18}O$ during the last 3500 yr. Significantly, growth rates (long-axis vertical extension calculated using the U-Th age data) correlate with $\delta^{18}O$ ratios in the Crag stalagmite (Fig. 5a). Dendrite-like textures (texture code 5, Fig. 4a) are clearly accompanied by shifts to elevated $\delta^{13}C$ (e.g. in the period c. 9000 to 6500 yr ago). However, high $\delta^{13}C$ is not always accompanied by dendrite-like textures (see discussion below) indicating either (i) that more than one process may be responsible for elevated $\delta^{13}C$ (see Baker *et al.*, 1997) or (ii)

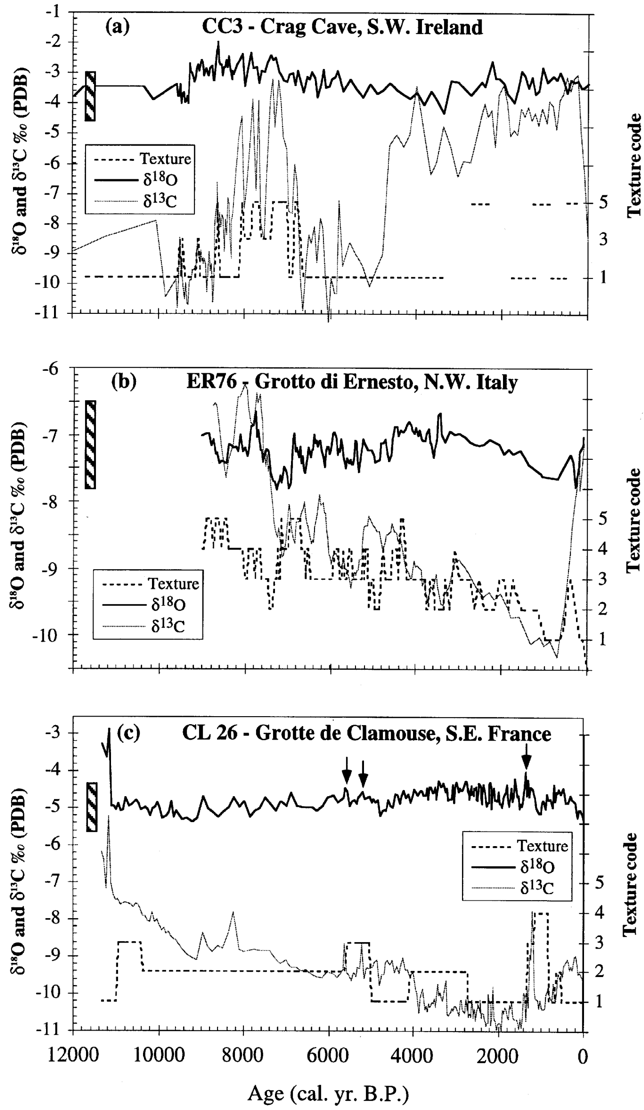

Fig. 4. Oxygen isotope (heavy black line), carbon isotope ratios (light stippled line) and calcite crystallography (dashed line) plotted against interpolated U–Th age for each stalagmite. $\delta^{18}O$ curves for the Ernesto and Clamouse stalagmite have been smoothed using a three-point moving average. Striped boxes on left–hand side of each diagram indicate range in $\delta^{18}O$ in present-day precipitates in each cave. All textures refer to calcite unless otherwise stated. Texture codes are as follows. *Crag*: 1 = columnar, 3 = Microcrystalline, 5 = Dendrite-like. *Grotta di Ernesto*: 1 = Columnar, 2 = columnar to microcrystalline, 3 = microcrystalline, 4 = microcrystalline to dendrite-like, 5 = dendrite-like. *Grotte de Clamouse*: 1 = Columnar, 2 = Equant calcite (after aragonite), 3 = Equant calcite and aragonite rays, 4 = Relict aragonite. Second-order shifts to higher $\delta^{18}O$ and $\delta^{13}C$ in the Clamouse stalagmite (arrows) reflect aragonite (texture codes 3 and 4).

that the threshold for a switch to dendrite-like conditions may be higher than that required to cause high $\delta^{13}C$. In general, the first-order oxygen isotope trend in the Crag sample appears to be strongly correlated with extension rate and appears to be independent of any textural variations. Exceptions are conspicuous second-order spikes to higher $\delta^{18}O$ (e.g. at c. 8700, 8100, 7800, 7400 and

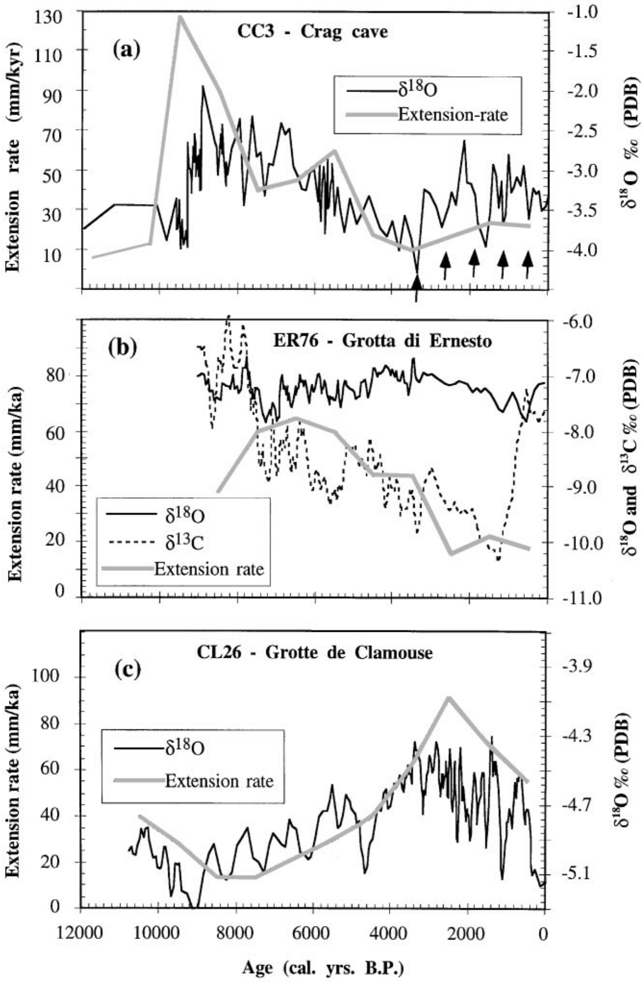

Fig. 5. Stalagmite growth-rates (long-axis extension rates) calculated from the U–Th age data for each of the three stalagmites is plotted as the thick grey line (left-hand axes). Also shown are the $\delta^{18}O$ values for each of the stalagmites (continuous black line) and the $\delta^{13}C$ curve for the Grotta di Ernesto stalagmite. Note that extension rates are relatively crude estimates because they are calculated at 1000 yr intervals and may mask larger short-lived growth-rate variations. Arrows in Fig. 5a denote the timing of wet episodes recorded by Scottish peat (Chambers et al., 1997). Many of these appear to coincide with second-order troughs in the Crag $\delta^{18}O$ curve.

2300 yr ago which appear to coincide with shifts to dendrite-like textures (Fig. 4a).

In the Grotta di Ernesto stalagmite $\delta^{18}O$ varies from -8.04 to $-6.22‰$. In general, the time-series oxygen isotope ratios vary independently of the textural and the carbon isotope variations. Unlike the stalagmite from Crag cave, there appears to be no correlation between $\delta^{18}O$ and extension rate (Fig. 5b). Instead $\delta^{13}C$ correlates roughly with extension rates. Some of the shifts to higher $\delta^{13}C$ are accompanied by textural changes (shifts to dendrite-like textures, Fig. 4b). Significantly, the first-order changes in $\delta^{13}C$ appear to be in phase at the Ernesto and Clamouse sites.

In the Grotte de Clamouse stalagmite, $\delta^{18}O$ varies from -5.3 to $-4.3‰$ and like the Crag stalagmite, high $\delta^{18}O$ appears to be accompanied by higher extension rates (Fig. 5c). With the exception of a single 'spike' near the base of the speleothem, $\delta^{18}O$ appears to be independent of $\delta^{13}C$ (Fig. 4c). In general, shifts to higher $\delta^{13}C$ are accompanied by non-equilibrium textures and/or relict aragonite (e.g. at c. 5500 and c. 1200 yr ago, Fig. 4c), but as in the other speleothems $\delta^{13}C$ can also change independent of textural variations.

Because of extension rate variations (Fig. 5), the time intervals between the (regularly spaced) stable isotope measurements vary along each speleothem. To facilitate comparisons between the different records, we also present the $\delta^{18}O$ data as averages of 200 yr time slices through the Holocene (Fig. 6a). Typically between 2 and 8 oxygen isotope analyses contribute to each of the 200 yr time-slice data-points. The $\delta^{18}O$ curves for the Ernesto and Clamouse sites show broadly similar first-order trends in the period between c. 7000 cal yr BP to the present day, with gradual increases in $\delta^{18}O$ from c. 7000 to 3500 cal yr BP followed by decreasing $\delta^{18}O$ towards the present-day (Fig. 6a). By contrast, the data for Crag appear to show first-order changes in the opposite direction (Fig. 6a).

In Fig. 6b the same data are shown as the difference between the average $\delta^{18}O$ for each 200 yr time slice and the Holocene mean $\delta^{18}O$ for each stalagmite. These diagrams suggest a broad tripartite division, with major first-order changes occurring at c. 7000 ± 200 yr and c. 3500 ± 200 yr ago. In the period prior to c. 7000 yr ago, the three curves differ significantly (see below). Note that in Fig. 6b the data for the Crag speleothem (solid curve) are plotted on the left-hand scale which is compressed by a factor of two compared with the right-hand scale (Grotta di Ernesto and Grotte de Clamouse). Thus, while the three curves show a first-order coherence for much of the Holocene, that for the Crag stalagmite (SW Ireland) tends to change in a direction opposite to that exhibited by the Clamouse and Ernesto stalagmites.

4.4. Tests for equilibrium conditions – the present-day

In high-humidity cave interiors where evaporation is negligible, it is often assumed that stalagmite calcite is deposited in isotopic equilibrium with the cave drip water, and under these conditions the $\delta^{18}O$ of the calcite reflects both the initial $\delta^{18}O$ of the drip water ($\delta^{18}O_p$) and the temperature dependent fractionation between the drip waters and the deposited calcite (e.g. Schwarcz, 1986). However, data from the ongoing isotope monitoring of present-day cave waters and modern precipitates for the cave sites studied here indicate that the oxygen isotope variations for recent calcites are much larger than isotope variations in the drip waters. Thus, in order to interpret correctly the oxygen isotope fluctuations in the

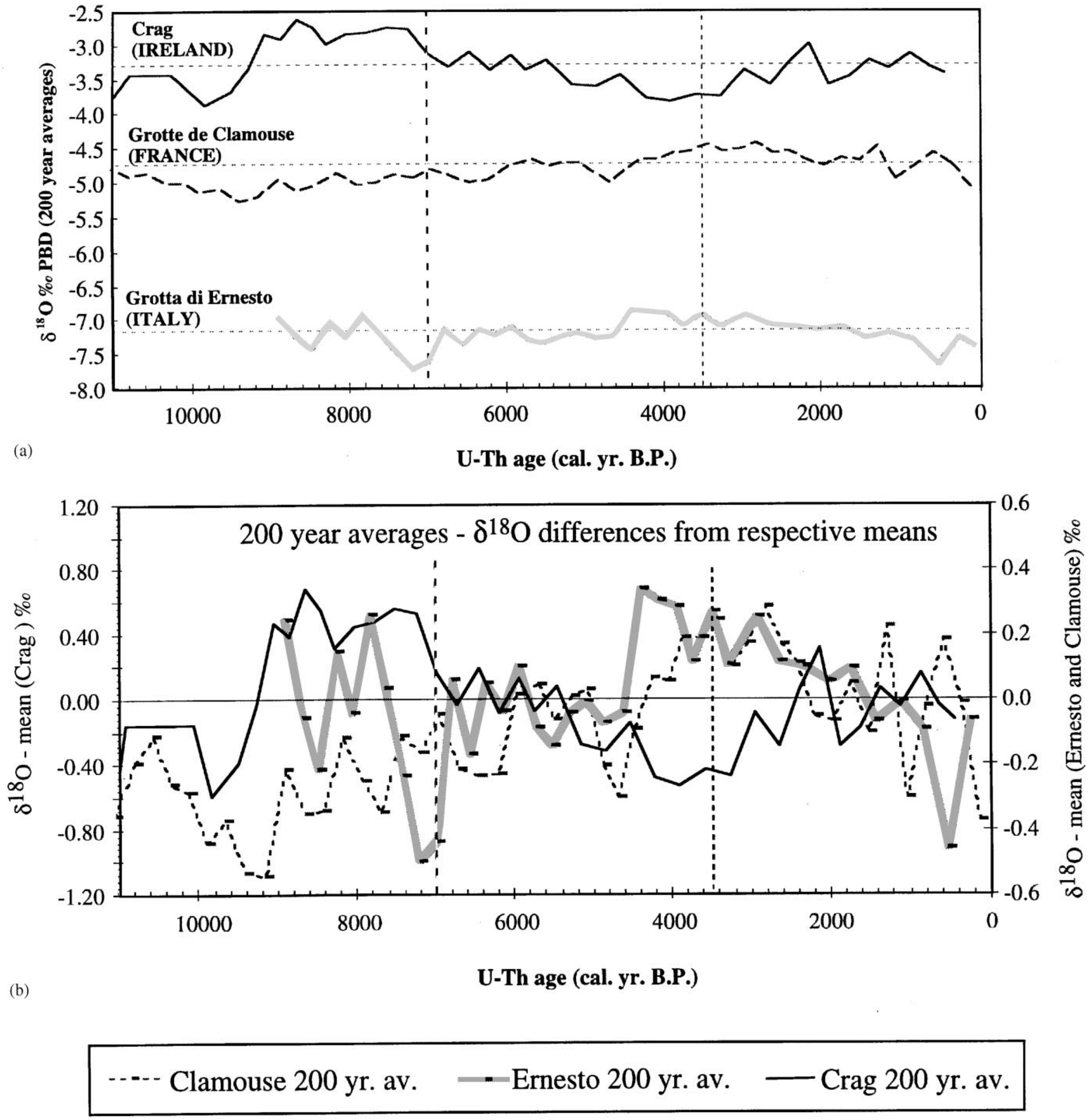

Fig. 6. (a) Oxygen isotope-time curves averaged over 200 yr time-slices. (b) $\delta^{18}O$ -time curves plotted as the difference between the averaged 200 yr time slices and the mean Holocene $\delta^{18}O$ for each speleothem.

calcite it is important to understand the site-specific factors that influence oxygen isotope ratios in the cave waters.

Isotope data for soda-straw tips which represent the past 10–50 yr (during which changes in the mean annual meteoric water signal were probably negligible), typically exhibit a range of 1–1.5‰ (Fig. 4). At Crag cave, recent precipitates which exhibit the highest $\delta^{18}O$ are monocrystalline rods (Jones and Kahle, 1993; Verrecchia and Verrecchia, 1994) and polycrystalline aggregates of rods arranged in a dendrite-like texture. These form opaque coatings and layers on cave walls and stalactites. Similar micro-rods are common in calcretes where they are ascribed to high supersaturation of the solution accompanied by evaporation and rapid precipitation of crystals (Verrecchia and Verrecchia, 1994). In caves, the same effects of rapid growth in disequilibrium conditions can be attained under a combination of rapid degassing and evaporation. These processes can result in enriched oxygen isotopes in the calcite (Gonzalez *et al*., 1992). There is some evidence that where dendrite-like textures occur in the time-series record, the $\delta^{18}O$ ratio is indeed displaced to higher values (Fig. 4a). From the observed differences in $\delta^{18}O$ in modern precipitates it appears that growth kinetics and/or drip rate effects are additional, second-order factors which can account for some of the high-frequency shifts to high $\delta^{18}O$ in the Crag time-series record. These effects are probably more important in the Grotta di Ernesto time-series data where water availability may exert a stronger control on $\delta^{18}O$ (see discussion below).

Having highlighted the possibility that second-order effects can influence the $\delta^{18}O$ signal. we now discuss in more detail the $\delta^{18}O$ values of modern precipitates in each cave. In Fig. 7, equilibrium calcite $\delta^{18}O$ values have been calculated for different $\delta^{18}O$ values in cave drip waters, for temperatures in the range 5–15°C using a modified version of the O'Neill *et al.* (1969) equation (Hays and Grossman, 1991). Also plotted on Fig. 7 are the ranges in $\delta^{18}O$ in selected recent calcite precipitates (soda-straws and incipient stalagmites) from the three caves, shown as the horizontal stippled bands labelled 'Crag precipitates', etc. Each band represents the range of means of $\delta^{18}O$ in different recent-precipitate morphologies (see caption of Fig. 7). The vertical bands in Fig. 7 represent our best estimate of the average $\delta^{18}O$ of present-day drip waters (weighted by precipitation amount) at each site based on data from a 2 yr

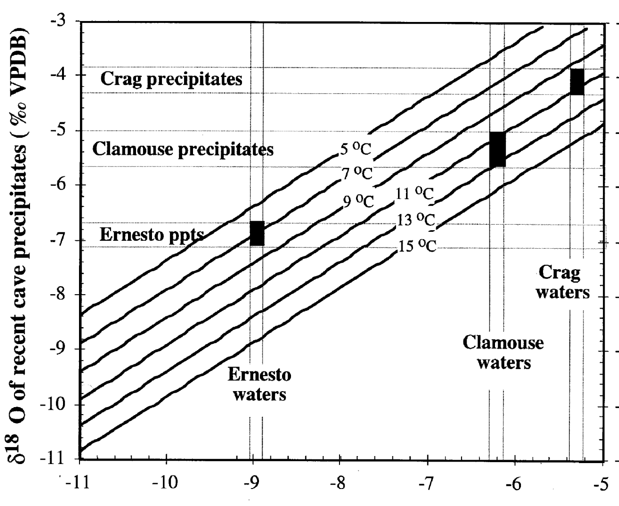

Fig. 7. Equilibrium test diagram. Diagonal lines are equilibrium temperature curves (5–15°C), calculated using the equation of Hays and Grossman (1991). The horizontal bands represent the range of averages (± 1 standard deviation) of modern soda straws and the upper surfaces scraped from incipient stalagmites. Exotic morphologies such as helectites, roof and wall-coatings and spray deposits were excluded because there is evidence that some of these may be affected by rapid degassing/kinetic fractionation processes.

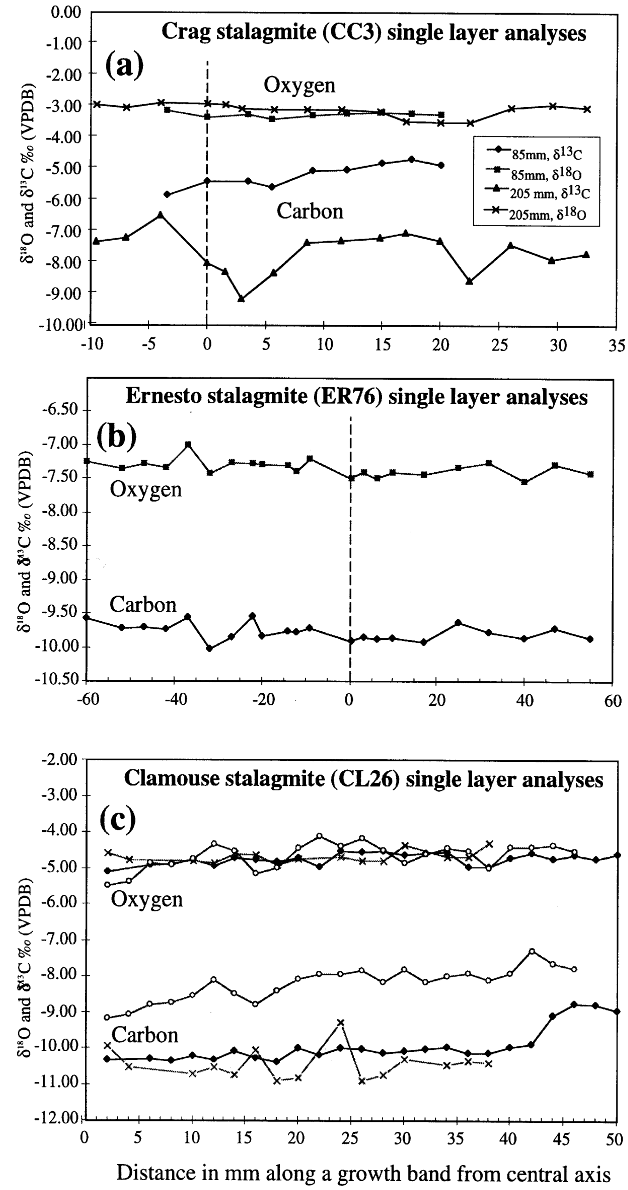

Fig. 8. Single-layer data for $\delta^{18}O$ and $\delta^{13}C$. (a) Crag; (b) Grotta di Ernesto; (c) Grotte de Clamouse;. The layer at 85 mm in the Crag stalagmite has a columnar texture while that at 205 mm has a microcrystalline texture. The single layer analysed in the Grotta di Ernesto stalagmite (at 22 mm) has a columnar texture. Single layers from the Grotte de Clamouse stalagmite were sampled at 44 mm (filled diamonds; columnar texture), 172 mm (crosses; columnar texture) and 401 mm (open symbols; equant calcite after aragonite). All measurements are in millimetres from the upper surface (youngest part) of each stalagmite.

monitoring programme, and in the case of Crag cave, additional data from the nearby IAEA station at Valentia. The areas defined by the intersection of the calcite and water $\delta^{18}O$ ranges (filled boxes), represent the temperatures implied by the data under conditions of equilibrium calcite deposition. In the case of Crag and Ernesto caves, these temperatures of c. 10.5 ± 1 and c. $7 \pm 1°C$ are in reasonable agreement with the present-day temperatures at these sites (10.4 ± 0.1 and $6.6 \pm 0.2°C$, respectively), indicating that calcite is being deposited under conditions which are at, or close to equilibrium. At Clamouse cave, there is a correlation between $\delta^{18}O$ and $\delta^{13}C$ in modern pool-deposits, incipient stalactites and stalagmites (not shown), indicating that within-cave evaporative effects which tend to increase both $\delta^{18}O$ and $\delta^{13}C$ have affected some of the modern precipitates. The precipitates with the lightest $\delta^{18}O$ are thus the most reliable for assessing present-day conditions. If these are used ($\delta^{18}O$ c. -5.7) the inferred temperature is c. 13.5°C, broadly similar to the present-day average annual temperature of c. 14.5°C.

4.5. Tests for equilibrium conditions in the past

The criteria for the recognition of equilibrium conditions have been well documented previously (Hendy, 1971; Schwarcz, 1986). Briefly, the conditions are (i) that $\delta^{18}O$ remains constant along a single growth layer while $\delta^{13}C$ varies irregularly, and (ii) that there is no correlation between $\delta^{18}O$ and $\delta^{13}C$ along a growth layer. Analyses of several single-layer samples drilled from the studied speleothems are presented in Fig. 8. Consistent sampling along on exactly the same growth bands was difficult, particularly where the bands were narrow. However, there is no evidence that $\delta^{18}O$ changes from crest to flanks, or for systematic changes in $\delta^{13}C$, or for covariation in $\delta^{13}C$ and $\delta^{18}O$. In summary, the Hendy (1971) criteria for isotopic equilibrium in speleothem calcite appear to be satisfied.

5. Discussion

5.1. Palaeoclimatic significance of $\delta^{18}O$ in different geographic settings

$\delta^{18}O$ in cave drip waters reflect (i) the $\delta^{18}O$ of precipitation and (ii) in semi-arid regions, evaporative processes which modify the $\delta^{18}O$ of precipitation at or near the surface above the cave. The spatial and seasonal variations of oxygen isotope ratios in present-day precipitation in Europe are quite well documented and understood (e.g. Dansgaard, 1964; Siegenthaler and Oeschger, 1980; Siegenthaler and Matter, 1983; Rozanski *et al*., 1982, 1992, 1993; Gat, 1996). An important feature is that the mean annual $\delta^{18}O$ of precipitation decreases systematically across Europe with increasing distance from the N. Atlantic ocean (Rozanski *et al*., 1993). This pattern is a consequence of several so-called 'effects' (e.g. latitude, altitude, distance from the sea, amount of precipitation, air temperature) reflecting the mass-fraction of moisture precipitated from clouds.

Under present-day conditions, the temperature dependence of $\delta^{18}O$ in rainfall ($d\delta^{18}O_p/dT$) is variable and is site dependent (Dansgaard, 1964; Rozanski *et al*., 1992, 1993), but it averages $+0.59 \pm 0.09‰\,°C^{-1}$ for European sites. Since this exceeds the $-0.24‰\,°C^{-1}$ calcite-water fractionation, a net shift to heavier O isotopes as a result of a temperature increase is expected (in the absence of other processes), i.e. a positive correlation between $\delta^{18}O$ and temperature. We note that such a simple relationship between drip water $\delta^{18}O$ and temperature is likely to hold true only for sites where near-surface evaporative effects are minimal.

On long timescales, factors other than temperature may also cause temporal variations in $\delta^{18}O_p$ even at sites where the temperature effect is dominant. These include; (i) changes in the $\delta^{18}O$ of the oceanic source region of precipitation, (ii) changes in the temperature difference between the ocean surface temperature in the vapour source area and the air temperature at the site of interest, (iii) long-term shifts in moisture sources or storm tracks, (iv) changes in the proportion of precipitation which has been derived from non oceanic sources, i.e. recycled from continental surficial waters (Koster *et al*., 1993) and (v) the so-called 'amount' effect. These will be discussed separately. First, we shall consider those effects which may have influenced $\delta^{18}O_p$ at Crag cave.

Decreases in the $\delta^{18}O$ of oceanic source regions in the early Holocene as a result of the collapse of ice-caps has been estimated to be only 0.3‰ between 10,000 and 5,000 cal yr BP (Stuiver *et al*., 1995). Most of this shift would have occurred early in the Holocene, and is clearly much smaller than the c. 1.5–2‰ shifts seen in the Crag speleothem in the early Holocene (Fig. 4a). The second factor listed above, changes in Holocene sea-surface temperatures (SSTs), is more difficult to assess. Attempts to reconstruct Holocene SSTs in the high latitude (north of 45°N) North Atlantic ocean have produced inconclusive results, with cores less than 100 km apart indicating contradictory trends (Ruddiman and Mix, 1993). On balance there is no compelling evidence for any significant regional-scale shifts in the high-latitude N. Atlantic SSTs in the Holocene, and GCMs typically assume constant SSTs as a boundary condition (Kutzbach and Guetter, 1986; Kutzbach *et al*., 1993). The third factor above, changes in storm paths/moisture sources, may be an important control on $\delta^{18}O_p$. Changes in moisture sources or storm tracks may advect air masses along warmer or cooler paths, thereby changing the degree of rainout and so the $\delta^{18}O$ of precipitation. The fourth factor listed above (changes in the moisture recycling ratio, R, defined as the fraction of a region's precipitation that had previously evaporated from non-oceanic sources) could in principle also change $\delta^{18}O_p$. In the present day, this effect is most noticeable during the N. hemisphere summer where it can account for about a third of the variability in mean annual $\delta^{18}O_p$ that is not explained by temperature (Koster *et al.*, 1993). The recycling ratio should increase with increasing air temperatures, and this would produce lower $\delta^{18}O_p$ thereby attenuating the temperature signal. The Crag site is on the western margin of the European landmass and there is little opportunity for evaporation of water from nonoceanic sources, but we cannot exclude the possibility that this effect had an influence on the O isotope records from Grotte de Clamouse and Grotta di Ernesto.

The fifth factor listed above, namely changes in the amount of precipitation, can change $\delta^{18}O_p$, and although this effect is best developed in tropical ocean island stations where the mean annual temperature exceeds 15°C (Dansgaard, 1964; Rozanski *et al.*, 1993) and is not expected to significantly affect the Crag site. In regions where there is a year-round positive balance between precipitation and evaporation (such as SW Ireland) the $\delta^{18}O$ of authigenic carbonate deposited in equilibrium with meteoric water (e.g. lacustrine or speleothem carbonate) is determined largely by two competing temperature-driven processes (e.g. Eicher and Siegenthaler, 1976; Schwarcz, 1986; Gascoyne, 1992). Thus, the $\delta^{18}O$ of rainwater ($\delta^{18}O_p$) typically *increases* with increasing air temperature (Dansgaard, 1964; Rozanski *et al.*, 1992, 1993), whereas the calcite-water $\delta^{18}O$ fractionation (constant at approximately $-0.24‰\,°C$) drives $\delta^{18}O$ in the opposite direction, and tends to attenuate the $\delta^{18}O_p$ signal.

Thus, for the Irish speleothem (CC3), the interpretation presented below is based on the premise that temperature effects were dominant, and that higher temperatures result in higher $\delta^{18}O$ in the calcite, i.e. that ($d\delta^{18}O_p/dT) > +0.24‰\,°C$). Perhaps the most persuasive evidence in favour of a temperature dominance at the Irish site is the relationship between stalagmite extension rate and $\delta^{18}O$. If the amount effect had been the dominant control on $\delta^{18}O$ during the Holocene, a negative correlation between extension rate and $\delta^{18}O$ would be predicted. The opposite is observed (Fig. 5), suggesting strongly that temperature was the dominant influence on $\delta^{18}O$. Independent constraints on the relationship between $\delta^{18}O$ in authigenic calcite and mean annual temperature for the region are best derived from the Lateglacial when temperature shifts were sufficiently large to produce unequivocal $\delta^{18}O$ signals. Thus, in Lateglacial lake cores from Loch Gur and Red Bog, some 40 km east of the Crag cave site in SW Ireland, the Younger Dryas cold event was characterised by a marked shift (by c. 3‰) to lower $\delta^{18}O$ (Ahlberg *et al.*, 1996) consistent with our inference that calcite $\delta^{18}O$ and temperature were positively correlated in the past. Significantly, this Younger Dryas $\delta^{18}O$ shift is consistent with a $d\delta^{18}O_p/dT$ of c. $+0.6‰\,°C^{-1}$, similar to the present-day European average. In addition, O isotope data for early Holocene British tufas (Andrews *et al.*, 1994) indicate that $\delta^{18}O$ was positively correlated with temperature in N. England in the early part of the Holocene (10,990 to 7390 cal yr BP). The latter record is too poorly dated (2 radiocarbon dates) to attempt detailed correlations with the data presented here but they offer independent constraints on the relationship between $\delta^{18}O$ and temperature in the NW Atlantic region during the early Holocene.

Shifts to lower $\delta^{18}O$ are also typically observed in the Younger Dryas lake carbonates of Switzerland (Eicher and Siegenthaler, 1976; Eicher *et al.*, 1981; Lotter *et al.*, 1992), France (Eicher and Siegenthaler, 1983), S. Germany (von Grafenstein *et al.*, 1994), Austria (Oeggl and Eicher, 1989) and Poland (Rozanski, 1987) confirming that $d\delta^{18}O_p/dT$ was also positive (and greater than $+0.24‰\,°C^{-1}$) in the Lateglacial of continental Europe. In a recently published detailed study of $\delta^{18}O$ in ostracod shells from Lake Amersee (S. Germany), von Grafenstein *et al.* (1996) have demonstrated convincingly that the present-day $\delta^{18}O$-temperature relationship of c. $0.6‰\,°C^{-1}$ has applied in mid-Europe for at least the last 200 yr, and probably for the Holocene. Futhermore, since stalagmite extension rates are strongly influenced by temperature (Baker *et al.*, 1998), the simplest explanation for the observed positive correlation between $\delta^{18}O$ and the extension rate in CC3 (Fig. 5a) is that temperature was the dominant control on $\delta^{18}O$ at this site. None of the other effects discussed above can readily produce the observed correlation between extension rate and $\delta^{18}O$. We believe therefore that we can justifiably argue that $\delta^{18}O$ was positively correlated with temperature at the Irish site during the Holocene.

By contrast, at Grotta di Ernesto (NW Italy) there is good evidence that changes in rainfall amount may affect the oxygen isotope signal. This effect arises for two reasons. First, there is direct evidence that the 'amount' effect is important locally in N. Italy in the present day (D'Amelio *et al.*, 1994). Secondly, on the basis of data from meteorological stations in NE Italy (Lavarone and Bieno stations, Trentino Province), we infer that a negative balance between precipitation and evaporation may occur during July and August at the Grotta di Ernesto site. Such a negative balance might result in near-surface evaporation effects which shifts $\delta^{18}O_p$ to higher values (Bar-Matthews *et al.*, 1996). This inference is supported by present-day observations within Grotta di Ernesto (Frisia, S., unpublished data). For example, the $\delta^{18}O$ of water dripping from fast-dripping soda-straws (sites G1 and F1 in the cave) is about 0.3‰ lower than slow dripping soda straws in this cave (G3 site) and stalactites (S3 site). The available data for the other sites do not show such clear relationships between drip rates and

$\delta^{18}O$. The absence of a correlation between $\delta^{18}O$ and the extension rate of the Grotta di Ernesto stalagmite also argues against a dominant $\delta^{18}O$–temperature relationship at this site.

At present Grotte de Clamouse is in a region where the potential evapotranspiration exceeds precipitation for at least part of the year. As discussed above, these conditions might cause enrichments in $\delta^{18}O$ during drier periods (Bar-Matthews *et al*., 1996, 1997). Meteorological data from Gignac station (approximately 6 km south of the Grotte de Clamouse site) suggest a moisture deficit for at least 4 months of the year (May–August inclusive) indicating that this site may be affected by near-surface evaporative effects, at least seasonally in the present day. However the observation that high $\delta^{18}O$ in the latter part of the Holocene is accompanied by higher rather than lower extension rates (Fig. 5) strongly suggests that this effect did not dominate the $\delta^{18}O$ signal. We argue therefore that temperature rather than precipitation amount was probably the dominant control on $\delta^{18}O$ in the Grotte de Clamouse stalagmite.

6. Palaeoclimatic interpretation

The preceding discussion has highlighted the need to understand the site-specific controls on $\delta^{18}O$ before attempting a palaeoclimatic interpretation of the data. Correlations with other proxy data, and some long-term $\delta^{18}O$ trends allow us to advance tentative climatic reconstructions for some key time-slices of the Holocene.

6.1. Climatic conditions in the early Holocene (c. 10,000–8,000 cal yr BP)

In the period around 10,000 cal yr BP, $\delta^{18}O$ in the Crag speleothem was relatively low (Fig. 4). The pollen-based reconstruction of Guiot *et al.* (1993) for c. 10,000 cal yr BP indicates that Europe was on average, some 2°C cooler than at 6800 cal yr BP, and the western seaboard of Europe in particular was several degrees cooler than at present. This marked cooling of the western seaboard region (low $\delta^{18}O$ at Crag) in the earliest part of the Holocene probably reflects the cooling influence of the Laurentide ice sheet, a key feature of several Holocene GCM simulations (Kutzbach and Guetter, 1986; Mitchell *et al*., 1988; Kutzbach *et al*., 1993). If this interpretation is correct, the sudden increase in $\delta^{18}O$ at c. 9300 cal yr BP in the Crag record (Fig. 4) may reflect rapid warming in response to increased melting of the Laurentide ice sheet. In the absence of the strong cooling influence of the ice sheet, temperatures in the region would have increased rapidly, because at this time the N. Hemisphere summer insolation had reached its Holocene maximum. The occurrence of dendrite-like textures (accompanied by $\delta^{13}C$ and $\delta^{18}O$ 'spikes', Fig. 4a) briefly at c. 8700 yr ago may indicate that relatively dry conditions prevailed for at least part of the early Holocene in SW Ireland.

In the early Holocene (c. 9300–7800 cal yr BP), the Alpine (Grotta di Ernesto) stalagmite records relatively high $\delta^{18}O$ and high $\delta^{13}C$ (Fig. 4b). This period coincides with an episode of low lake levels in the Jura and French sub-Alpine ranges, glacier retreats in the Austrian and Swiss Alps (Magny, 1992, 1995) indicative of dry conditions. In NW Italy, studies of pollen and glacier fluctuations (e.g. Baroni and Orombelli, 1996; Burga 1991) suggest relatively warm conditions in the period c. 10,000 to c. 6000 cal yr BP. Evidence from the Rutor glacier in the western Italian Alps (Porter and Orombelli, 1985) indicates that significant retreat occurred before 8400 ^{14}C yr BP, and that the glacier remained in a contracted state until at least 6275 ^{14}C yr BP (c. 9400–7200 cal yr BP). Thus, the high $\delta^{18}O$ in the Italian (Grotte de Ernesto) stalagmite prior to c. 7800 cal yr BP is interpreted as reflecting dry or dry-warm conditions.

In the early Holocene, $\delta^{18}O$ in the Grotte de Clamouse (SE France) stalagmite was low relative to its Holocene average, and was c. 0.8‰ lower than at 6000 cal yr BP. We note that in the period between about 10,000 $\pm$ 1,500 y and 7000 $\pm$ 1500 yr ago speleothems in Soreq cave, Israel, were deposited relatively slowly and they exhibit the lowest $\delta^{18}O$ and the highest $\delta^{13}C$ values of the entire Holocene (Bar-Matthews *et al*., 1997). Similar first-order trends are observed in this study for the speleothems from Clamouse and Ernesto, with the sharp $\delta^{13}C$ peak at c. 8200 $\pm$ 200 cal yr BP in both speleothems (Fig. 4) coinciding with the latest of two peaks seen in the Soreq speleothems 2–3 and 2–*n* (see Figs. 3 and 4 of Bar-Matthews *et al*., 1997). The latter authors interpreted the relatively low $\delta^{18}O$ values of the Soreq speleothems deposited in the period between 10,000 $\pm$ 1500 and 7000 $\pm$ 1500 cal yr BP as reflecting relatively wet conditions. This interpretation was based on present-day observed relationship between rainfall amount and weighted mean $\delta^{18}O$ in rainfall over several years, and is consistent with other palaeoenvironmental indicators for the region (Bar-Matthews *et al*., 1997). Taking into account the relationship between $\delta^{18}O$ and extension rate in the Grotte de Clamouse stalagmite (Fig. 5c), we interpret its early Holocene low $\delta^{18}O$ as primarily reflecting cooler conditions than in the second half of the Holocene. The extent to which wetter conditions may also have contributed to the low $\delta^{18}O$ in the early Holocene remains difficult to assess. While such a control would not be inconsistent with the present-day observations that seasonal moisture deficits occur (allowing evaporation accentuated 'amount' effects) it cannot by itself account easily for the low early Holocene extension rates.

6.2. Climatic conditions in the mid-Holocene (c. 8000–3500 cal yr BP)

At 7800 cal yr BP, $\delta^{18}O$ in the Crag speleothem was high, reflecting continued relatively warm conditions on the European western seaboard (Guiot *et al*., 1993; Cheddadi *et al*., 1997). This early Holocene period of elevated $\delta^{18}O$ (Figs. 4 and 5) marks the long recognised warm 'Atlantic' period in Ireland (Jessen, 1949). From c. 7800 to 3500 cal yr BP, $\delta^{18}O$ in the Crag speleothem exhibits a gradual decrease which we interpret as a cooling trend. Significantly, this period of declining $\delta^{18}O$ was accompanied by a gradual decline in extension rate (Fig. 5a) supporting the interpretation that $\delta^{18}O$ dominantly reflects temperature at this site. Dendrite-like textures occur intermittently between c. 8200 and 6700 cal yr BP (accompanied by high $\delta^{13}C$ and locally elevated $\delta^{18}O$, Fig. 4a). By analogy with textural observations on modern cave precipitates, the occurrence of dendrite-like textures is best interpreted as reflecting decreased drip-water availability. Thus, while some of the second-order shifts to high $\delta^{18}O$ in this part of the Crag $\delta^{18}O$ curve may be attributed to short-lived dry events the first-order trend is interpreted in terms of temperature changes. In the following three millennia (from c. 6700 to c. 3300 cal yr BP) columnar calcite was deposited in the Crag stalagmite, and so we infer that drip rates (and by inference rainfall) remained relatively high for this part of the Holocene in SW Ireland.

From c. 7800 to 6900 cal yr BP, the Alpine speleothem (Grotta di Ernesto) exhibits a well-defined episode of low $\delta^{18}O$. During this period $\delta^{18}O$ reached the lowest value of the entire Holocene at this site. We interpret this as reflecting a wet phase (amount effect dominant at this site). We note that this interval coincides with the Cerin phase of high lake levels in the Jura and French Alpine ranges (from 7790 to 6850 cal yr BP, Magny, 1992, 1995), treeline lowering in the Swiss Alps (Burga, 1988), glacier advances in the Swiss and Austrian Alps (Magny, 1995) and increased discharge from the Vistula (Starkel, 1991). The extent to which this early to mid-Holocene lowering of $\delta^{18}O$ might reflect a cooling event (in addition to increased rainfall) is difficult to assess. We note that the 6800 cal yr BP (6,000 ^{14}C yr BP, Stuiver and Reimer, 1993) snapshot pollen reconstructions imply reduced winter temperatures in this region (Guiot *et al*., 1993; Cheddadi *et al*., 1997) and the Alpine speleothem might be expected to record these if (as expected) recharge occurred predominantly during the winter months. However, the relatively high extension rates (Fig. 5b) may indicate that temperatures remained relatively high.

The Clamouse curve exhibits several small $\delta^{18}O$ fluctuations in this part of the early Holocene, but is typically lower than that of the late Holocene (Fig. 4c), consistent with evidence for cooler and/or wetter conditions around the Mediterranean at that time (e.g. Bar-Matthews *et al*., 1997). The relatively low $\delta^{18}O$ in the Grotte de Clamouse curve at this time is also consistent with indications from the 6800 calendar year snapshot pollen-based simulation (e.g. Cheddadi *et al*., 1997) that low elevation sites in the N. Mediterranean region experienced the strongest decline in winter temperatures. The latter interpretation requires that recharge occurred predominantly in winter (i.e. that a 'Mediterranean'-type climate prevailed at that time).

6.3. Climatic conditions in the late Holocene (c. 3500 cal yr BP to the present-day)

The pollen-based reconstruction (Guiot *et al*., 1993) for the western seaboard of Europe indicates temperatures at 3000 yr ago broadly similar to those of the present day, yet all of the speleothems exhibit changes in $\delta^{18}O$ since this time. During the past 3500 yr the Crag speleothem exhibits an irregular trend to higher $\delta^{18}O$, probably indicative of a reversal of the cooling trend between c. 7800 to 3500 cal yr BP and the onset of warmer conditions. Prominent $\delta^{18}O$ 'spikes' in this part of the curve (e.g. at c. 2200 yr ago) are associated with the development of dendrite-like textures, and so in part may also reflect relatively dry conditions. Episodes of relatively wet conditions centered on c. 3,455, c. 2600, c. 1930, c. 1095 and c. 540 yr BP have been inferred from a study of Scottish peat (Chambers *et al*., 1997). There is evidence that all five of these episodes are recorded by low $\delta^{18}O$ values in the Crag stalagmite (see arrows, Fig. 5a).

By contrast, the Alpine site exhibits a decrease in $\delta^{18}O$ during the period since 3500 yr ago. This shift to lower $\delta^{18}O$ in the last three millennia of the Holocene (accompanied by declining extension rates, Fig. 5b) might be cautiously interpreted as some combination of cooler and/or wetter conditions. This inference is supported by the dominance of more equilibrium textures (Fig. 4b), related to relatively low supersaturation (higher rainfall, lower residence time in the aquifer, lower concentrations of impurities).

The Grotte de Clamouse stalagmite exhibits an irregular decrease in $\delta^{18}O$ during the period since 3400 yr ago. This trend is accompanied by a decline in stalagmite extension rates (Fig. 5c) suggesting a cooling trend. A marked 'spike' in $\delta^{18}O$ at c. 1200 yr ago coincides with the development of nonequilibrium texture types (Fig. 4c), and a change in mineralogy from calcite to aragonite which probably indicates a relatively dry phase (Railsback *et al*., 1994; Frisia *et al*., 1997). Despite the trend to lower $\delta^{18}O$ in the last three millennia, the Clamouse stalagmite exhibits higher $\delta^{18}O$ for much of the period between c. 3500 and 1500 cal yr BP compared with that in the early-mid Holocene, suggesting warmer and/or drier conditions.

6.4. Possible orographic effects

The c. 2.5‰ offset between the Grotta di Ernesto and Grotte de Clamouse $\delta^{18}O$ curves is interpreted as reflecting the elevation difference between the two sites. The Ernesto cave is at an elevation of 1165 m above sea level, some 1090 m higher than the Clamouse site. It has been well documented that $\delta^{18}O$ in present-day precipitation decreases with increasing altitude, reflecting progressive distillations of water vapour masses at lower temperatures. In the present day, the rate of decrease in $\delta^{18}O$ with increasing altitude is typically in the range −0.16–0.4‰ per 100 m in Europe, with a value of −0.26‰ per 100 m typical of the Swiss plateau and the W. Alps (Siegenthaler and Oeschger, 1980). The c. 2.5‰ offset between the Clamouse and Ernesto curves is consistent with these present-day rates. The observation that the first-order features of the Ernesto and Clamouse $\delta^{18}O$ curves vary in parallel indicates that (i) *differential* cooling or warming between the sites was negligible on millennia time-scales and (ii) no significant changes in $d\delta^{18}O_p/dT$ occurred between the sites on these time-scales, implying either that large-scale reorganisations of storm paths did not occur, or that they were relatively short-lived (<< 1000 yr).

7. Conclusions

The relationship between $\delta^{18}O$ and extension rate in the Crag stalagmite (Irish site) strongly supports our inference that there was a positive correlation between speleothem $\delta^{18}O$ and temperature ($d\delta^{18}O_p/dT$ $> 0.24‰\ °C^{-1}$) at this site through the Holocene. We conclude from the first-order trends that temperatures in SW Ireland were relatively high in the early Holocene, followed by a period of progressively cooler conditions from c. 7800 to 3500 cal yr BP. We tentatively conclude that a partial return to higher $\delta^{18}O$ and higher extension-rates during the last three millennia reflects a gradual temperature increase. This trend since 3500 yr ago was punctuated by several second-order decreases in $\delta^{18}O$ and rapid textural changes which appear to coincide with episodes of increased wetness as recorded by Scottish peat profiles (Chambers *et al*., 1997). The peat data indicate shifts to wetter conditions at c. 3455, 2600, 1930, 1095 and 540 yr before present. All of these events are recorded by the Crag speleothem as $\delta^{18}O$ minima (vertical arrows, Fig. 5a). With the exception of the 1930 yr BP event (some 300 y later in our record, but probably within dating uncertainty), the timing of the $\delta^{18}O$ minima agree remarkably well (± 50 yr) with the approximate dates for these wet events given by Chambers *et al*. (1997). Since lower $\delta^{18}O$ in the Crag speleothem predominantly reflects cooling (the amount effect is weak at this site) we infer that these late Holocene climate fluctuations were shifts to colder/wetter conditions.

Holocene $\delta^{18}O$ variations at the Grotte de Clamouse (SE France) and Grotta di Ernesto (NE Italy) stalagmites were smaller than those at Crag and the first-order $\delta^{18}O$ trends were typically in the opposite direction for much of the Holocene. Unlike the Crag stalagmite, that from Grotta di Ernesto does not exhibit a correlation between extension rate and $\delta^{18}O$, suggesting that processes other than temperature (precipitation amount?) may have exerted a strong influence on $\delta^{18}O$. A distinct episode of low $\delta^{18}O$ from c. 7800 to 6900 cal yr BP in the Grotta di Ernesto stalagmite is interpreted as reflecting the Cerin wet phase. In the Grotte de Clamouse stalagmite, $\delta^{18}O$ and extension rates are correlated, suggesting that temperature may have been an important first-order control on $\delta^{18}O$ variations at this site. The extent to which this may have been modified by the so-called 'amount' effect or by near-surface evaporative effects remains difficult to assess but these are unlikely to have been the dominant control. There is good evidence that some second-order shifts to higher $\delta^{18}O$ (and higher $\delta^{13}C$) in this stalagmite reflect mineralogical changes (the presence of aragonite and relict aragonite) that may in turn reflect short-lived dry episodes.

In conclusion, palaeoclimatic interpretations of $\delta^{18}O$ signals in time-series speleothem calcite requires an understanding of both regional and local (site-specific) effects. In general it is difficult to separate the effects of rainfall variations from temperature variations at sites where there may have been a negative balance between precipitation and evapotranspiration for at least part of the year (e.g. Grotte de Clamouse and Grotta di Ernesto). In principle, warm-dry conditions can produce higher $\delta^{18}O$ and cold-wet conditions can produce lower $\delta^{18}O$ at these sites, but other combinations could conceivably cancel out the isotope signal. However, our observation that $\delta^{18}O$ and stalagmite extension rates are correlated at some sites (e.g. in the Crag and Grotte de Clamouse stalagmites of this study) may offer a means to discriminate between temperature and rainfall-amount variations. Correlations between $\delta^{18}O$ and the accompanying carbon isotope and textural signals also aids in unravelling the temperature vs rainfall effects.

The principal conclusion is that during the Holocene there has been significant decoupling between the Atlantic (Crag) and Mediterranean seaboard (Grotte de Clamouse) sites. For much of the Holocene the long-term first-order trends in both $\delta^{18}O$ and stalagmite extension rates were in opposite directions at these sites with an important inflexion occurring at c. 3500 yr ago. Obviously these conclusions must remain tentative until further studies of stalagmites from these and other sites in these regions have been completed. There appears to have been little or no differential cooling or warming between the southern Alpine and the Mediterranean seaboard site on millennia time-scales during the Holocene.

Acknowledgements

The authors gratefully acknowledge support from the E.U. Environment Programme (Contract EV5V-CT94-0509) to study 'Holocene-Late Pleistocene high-resolution climate reconstruction from continental carbonates.' FMcD wishes to acknowledge receipt of the Bank of Ireland Newman Scholarship at UCD in the early stages of this project. Peter van Calsteren and Mabs Gilmour are thanked for their help in the radiogenic isotope laboratory at the Open University. The authors wish to thank the owners and custodians of the caves at Crag (the Geaney family), Clamouse (P. Dubois) and Grotta di Ernesto (G. Gasperini) for their kind co-operation. S.F. is grateful to D. Aquilano, R.J. Reeder and W. Dreybrodt for profitable discussions of the crystallographic data. Thoughtful and constructive reviews by Dr Keith Barber and an anonymous reviewer are gratefully acknowledged. Professor Jim Rose is thanked for constructive editorial advice.

References

Ahlberg, K., Almgren, E., Wright, H. E., Ito, E., & Hobbie, S. (1996). Oxygen-isotope record of late-glacial climatic change in western Ireland. *Boreas*, *25*, 257–267.

Alley, R. B., Mayewski, P. A., Sowers, T., Stuiver, M., Taylor, K. C., & Clark, P. U. (1997). Holocene climate instability: A prominent, widespread event 8200 yr. ago. *Geology*, *25*, 483–486.

Andrews, J. E., Pedley, H. M., & Dennis, P. F. (1994). Stable isotope record of palaeoclimatic change in a British Holocene tufa. *The Holocene*, *4*, 349–355.

Atkinson, T. C., Briffa, K. R., & Coope, G. R. (1987). Seasonal temperatures in Britain during the past 22,000 years, reconstructed using beetle remains. *Nature*, *325*, 587–592.

Baker, A., Smart, P. L., Edwards, R. L., & Richards, D. A. (1993). Annual growth banding in a cave stalagmite. *Nature*, *364*, 518–520.

Baker, A., Ito, E., Smart, P. L., & McEwan, R. F. (1997). Elevated and variable values of ^{13}C in speleothems in a British cave system. *Chemical Geology*, *136*, 263–270.

Baker, A., Genty, D., Dreybrodt, W., Barnes, W. L., Mockler, N. J., & Grapes, J. (1998). Testing theoretically predicted stalagmite growth rate with recent annually laminated samples: Implications for past stalagmite deposition. *Geochimica Cosmochimica Acta*, *62*, 393–404.

Barber, K. E., Chambers, F. M., Maddy, D., Stoneman, R., & Brew, J. S. (1994). A sensitive high-resolution record of late Holocene climatic change from a raised bog in northern England. *The Holocene*, *4*, 198–205.

Bar-Matthews, M., Ayalon, A., Matthews, A., Sass, E., & Halicz, L. (1996). Carbon and oxygen isotope study of the active water-carbonate system in a karstic Mediterranean cave: implication for palaeoclimate research in semiarid regions. *Geochimica Cosmochimica Acta*, *60*, 337–347.

Bar-Matthews, M., Ayalon, A., & Kaufman, A. (1997). Late Quaternary palaeoclimate in the Eastern Mediterranean region from stable isotope analysis of speleothems at Soreq cave, Israel. *Quaternary Research*, *47*, 155–168.

Baroni, C., & Orombelli, G. (1996). The Alpine "Iceman" and Holocene climatic change. *Quaternary Research*, *46*, 78–83.

Boistelle, R. (1982). Impurity effects in crystal growth from solution. In B. Mutaftschief (Ed.), *Interfacial aspects of phase transformation* (pp 621–638). Dordrecht: Reidel.

Borsato, A., Spiro, B., Longinelli, A., & Heaton, T. (1996). Isotopic composition of present-day Alpine speleothems from Trentino (N.W. Italy): A key for palaeoclimatic interpretations in ancient speleothems. In S.E. Lauritzen (Ed.), *Climate change*: *The Karst record* (Vol. 2, pp 16–17). Bergen: KWI Spec. Publisher.

Broecker, W. S. (1991). The great ocean conveyor. *Oceanography*, *4*, 79–89.

Burga, C. A. (1988). Swiss vegetation history during the last 18,000 years. *New Phytologist*, *110*, 581–602.

Burga, C. (1991). Vegetation history and palaeoclimatology in the Middle Holocene: pollen analysis of alpine peat bog sediments covered formerly by the Rutor glacier, 2510 m. (Aosta Valley, Italy). *Global Ecology and Biogeography Letters*, *1*, 143–150.

Chambers, F. M., Barber, K. E., Maddy, D., & Brew, J. (1997). A 5,500-year proxy-climate and vegetation record from blanket mire at Talla Moss, Borders, Scotland. *The Holocene*, *7*, 391–399.

Cheddadi, R., Yu, G., Guiot, J., Harrison, S. P., & Prentice, I. C. (1997). The climate of Europe 6,000 years ago. *Climate Dynamics*, *13*, 1–9.

COHMAP Members (1988). Climatic changes of the last 18,000 years: Observations and model simulations. *Science*, *263*, 1043–1052.

D'Amelio, L., Flora, O., & Longinelli, A. (1994). Environmental isotope data: Oxygen isotope concentration in precipitation in N-E Italy (Friuli-Venezia Giulia). *Mineralogia Petrografia Acta*, *37*, 113–124.

Dansgaard, W. (1964). Stable isotopes in precipitation. *Tellus*, *16*, 436–468.

Dansgaard, W., Johnsen, S. J., Clausen, H. B., Dahl-Jensen, D., Gundestrup, N. S., Haller, C. U., Hvidberg, C. S., Steffensen, J. P., Sveinbjörnstottir, A. E., Jouzel, J., & Bond, G. (1993). Evidence for general instability of past climate from a 250-ka ice core record. *Nature*, *364*, 218–220.

Dickson, J. A. D. (1991). Disequilibrium carbon and oxygen isotope variations in natural calcite. *Nature*, *353*, 842–844.

Dickson, J. A. D. (1997). Synchronous intercrystalline $\delta^{13}C$ and $\delta^{18}O$ differences in natural calcite crystals. *Mineralogical Magazine*, *61*, 243–248.

Eicher, U., & Siegenthaler, U. (1976). Palynological and oxygen isotope investigations on late-glacial sediment cores from Swiss lakes. *Boreas*, *5*, 109–117.

Eicher, U., Siegenthaler, U., & Wegmüller, S. (1981). Pollen and oxygen isotope analyses on late- and post-glacial sediments of the Torbière de Chirens (Dauphiné, France). *Quaternary Research*, *15*, 160–170.

Eicher, U., & Siegenthaler, U. (1983). Stable isotope of oxygen and carbon in the carbonate sediments of Lac de Siguret (Hautes-Alpes, France). *Ecologia Mediterranea*, *9*, 49–53.

Frisia, S., & Wenk, H. R. (1994). Replacement of aragonite by calcite in the sediments from the San Cassiano Formation (Italy). *Journal of Sedimentary Petrology*, *55*, 159–170.

Frisia, S. (1996). Petrographic evidence of diagenesis in speleothems: Some examples. *Speleochronos*, *7*, 21–30.

Frisia, S., Borsato, A., Fairchild, I. J., & Longinelli, A. (1997). Aragonite precipitation at Grotte de Clamouse (Herault, France): Role of magnesium and driprate. Proceedings of the 12th International Congress of Speleology (pp. 247–250). Switzerland: La Chaux-de-Fonds.

Gascoyne, M. (1992). Palaeoclimate determination from cave calcite deposits. *Quaternary Science Reviews*, *11*, 609–632.

Gat, J. R. (1996). Oxygen and hydrogen isotopes in the hydrologic cycle. *Annual Reviews of Earth and Planetary Sciences*, *24*, 225–262.

Goede, A., Green, D. C., & Harmon, R. S. (1986). Late Pleistocene palaeotemperature record from a Tasmanian speleothem. *Australian Journal of Earth Sciences*, *33*, 333–342.

Gonzalez, L. A., Carpenter, S. J., & Lohmann, K. C. (1992). Inorganic calcite morphology: Roles of fluid chemistry and fluid flow. *Journal of Sedimentary Petrology*, *62*, 383–399.

Grootes, P. M. (1993). Interpreting continental oxygen isotope records. In P. K. Swart, K. C. Lohmann, J. McKenzie, & S. Savin (Eds.), *Climate change in continental isotopic records* (pp. 36–47) Geophysical Monograph, Vol. 78, Washington, DC: American Geophysical Union.

Guiot, J., Harrison, S. P., & Prentice, I. C. (1993). Reconstruction of Holocene precipitation patterns in Europe using pollen and lake level data. *Quaternary Research*, *40*, 139–149.

Hall, N. M. J., & Valdes, P. J. (1997). A GCM simulation of the climate 6,000 years ago. *Journal of Climate*, *10*, 3–17.

Harrison, S. P., Yu, G., & Tarasov, P. E. (1996). Late-quaternary lake-level record from northern Eurasia. *Quaternary Research*, *45*, 139–159.

Hays, P. D., & Grossman, E. L. (1991). Oxygen isotopes in meteoric calcite cements as indicators of continental palaeoclimate. *Geology*, *19*, 441–444.

Hendy, C. H. (1971). The isotopic geochemistry of speleothems 1. The calculation of the effects of the different modes of formation on the isotopic composition of speleothems and their applicability as palaeoclimatic indicators. *Geochimica Cosmochimica Acta*, *35*, 801–824.

Huntley, B., & Prentice, I. C. (1993). Holocene vegetation and climates in Europe. In H. E. Wright Jr., J. E. Kutzbach, T. E. Webb III, W. F. Ruddiman, F. A. Street-Perrott, & P. J. Bartlein (Eds.), *Global climates since the last glacial maximum* (pp. 136–168). Minneapolis: University of Minnesota.

Jessen, K. (1949). Studies in late quaternary deposits and flora history of Ireland. *Proceedings of the Royal Irish Academy*, *B52*, 85–290.

Jones, B., & Kahle, C. F. (1993). Morphology, relationship and origin of fiber and dendritic calcite crystals. *Journal of Sedimentary Petrology*, *63*,1018–1031.

Kendall, A. C., & Broughton, P. L. (1978). Origin of fabric in speleothems composed of columnar calcite crystals. *Journal of Sedimentary Petrology*, *48*, 519–538.

Koster, R. D., de Valpine, D. P., & Jouzel, J. (1993). Continental water recycling and $H_2^{18}O$ concentrations. *Geophysical Research Letters*, *20*, 2212–2218.

Kutzbach, J. E., & Guetter, P. J. (1986). The influence of changing orbital parameters and surface boundary conditions on climate simulations for the past 18,000 years. *Journal of Atmospheric Sciences*, *43*, 1726–1759.

Kutzbach, J. E., Guetter, P. J., Behling, P. J., & Selin, R. (1993). Simulated climate changes: Results of the COHMAP climate-model experiments. In H. E. Wright Jr., J. E. Kutzbach, T. E. Webb III, W. F. Ruddiman, F. A. Street-Perrott, & P. J. Bartlein (Eds.), *Global climates since the Last Glacial maximum* (pp. 24–93). Minneapolis: University of Minnesota.

Lamb, H. F., Gasse, F., Benkaddour, A., El Hamout, N., van der Kaars, S., Perkins, W. T., Pearce, N. J., & Roberts, C. N. (1995). Relation between century-scale Holocene arid intervals in tropical and temperate zones. *Nature*, *373*, 134–137.

Lauritzen, S. E. (1995). High-resolution palaeotemperature proxy record for the last interglaciation based on Norwegian speleothems. *Quaternary Research*, *43*, 133–146.

Lotter, A. F., Eicher, U., Siegenthaler, U., & Birks, H. J. B. (1992). Late-glacial climatic oscillations as recorded in Swiss lake sediments. *Journal of Quaternary Science*, *7*, 187–204.

Magny, M. (1992). Holocene lake level fluctuations in Jura and the northern subalpine ranges, France: Regional pattern and climatic implications. *Boreas*, *21*, 319–334.

Magny, M. (1995). Successive oceanic and solar forcing indicated by Younger Dryas and early Holocene climatic oscillations in the Jura. *Quaternary Research*, *43*, 279–285.

McCabe, A. M. (1987). Quaternary deposits and glacial stratigraphy in Ireland. *Quaternary Science Reviews*, *6*, 259–299.

Mitchell, J. F. B., Grahame, N. S., & Needham, K. J. (1988). Climate simulations for 9,000 years before present: seasonal variations and the effects of the Laurentide ice sheet. *Journal of Geophysical Research*, *93*, 8283–8303.

Nesje, A., & Kvamme, M. (1991). Holocene glacier and climate variations in western Norway: Evidence for early Holocene glacier demise and multiple neoglacial events. *Geology*, *19*, 610–612.

O'Brien, S. R., Mayewski, P. A., Meeker, L. D., Meese, D. A., Twickler, M. S., & Whitlow, S. I. (1995). Complexity of Holocene climate as reconstructed from Greenland ice core. *Science*, *270*, 1962–1964.

Oeggl, K., & Eicher, U. (1989). Pollen and oxygen isotope analyses of late- and postglacial sediments from the Schwemm raised bog near Walchsee in Tirol, Austria. *Boreas*, *18*, 245–253.

O'Neill, J. R., Clayton, R. N., & Mayeda, T. K. (1969). Oxygen isotope fractionation of divalent metal carbonates. *Journal of Chemical Physics*, *30*, 5547–5558.

Paquette, J., Ward, B., & Reeder, R. (1993). Compositional zoning and crystal growth mechanisms in carbonates: A new look at microfabrics imaged by cathodoluminescence microscopy. In R. Rezak, & D. L. Lavoie (Eds.), *Carbonate microfabrics* (pp. 243–252) New York: Springer.

Paquette, J., & Reeder, R. J. (1990). New type of compositional zoning in calcite: Insights into crystal-growth mechanisms. *Geology*, *18*, 1244–1247.

Porter, S. C., & Orombelli, G. (1985). Glacier contraction during the middle Holocene in the Western Italian Alps: Evidence and implications. *Geology*, *13*, 296–298.

Railsback, L. B., Brook, G. A., Chen, J., Kalin, R., & Fleisher, C. J. (1994). Environmental controls on the petrology of a Late Holocene speleothem from Botswana with annual layers of aragonite and calcite. *Journal Sedimentary Research*, *A64*, 147–155.

Reeder, R. J. (1996). Interaction of divalent Cobalt, Zinc, Cadmium, and Barium with the calcite surface during layer growth. *Geochimica Cosmochimica Acta*, *60*, 1543–1552.

Rozanski, K., Sonntag, C., & Munnich, K. O. (1982). Factors controlling stable isotope composition of European precipitation. *Tellus*, *34*, 142–150.

Rozanski, K. (1987). The ^{18}O and ^{13}C isotope investigations of carbonate sediments from the Lake Strazym (Brodnica Lake District). *Acta Palaeobotonica*, *27*, 227–282.

Rozanski, K., Araguás-Araguás, L., & Gonfiantini, R. (1992). Relation between long-term trends of oxygen-18 isotope composition of precipitation and climate. *Science*, *258*, 981–985.

Rozanski, K., Araguás-Araguás, L., & Gonfiantini, R. (1993). Isotopic patterns in modern precipitation. In P.K. Swart, K.C. Lohmann, J. McKenzie, & S. Savin (Eds.), *Climate change in continental isotopic records* (pp. 1–36). Geophysical Monograph, Vol. 78, Washington, DC: American Geophysical Union.

Ruddiman, W. F., & McIntyre, A. (1981). The mode and mechanism for the last deglaciaton: Oceanic evidence. *Quaternary Research*, *16*, 125–134.

Ruddiman, W. F., & Mix, A. C. (1993). The North and Equatorial Atlantic at 9000 and 6000 yr BP. In H. E. Wright Jr., J. E. Kutzbach, T. E. Webb III, W. F. Ruddiman, F. A. Street-Perrott, & P. J. Bartlein, (Eds.), *Global climates since the Last Glacial maximum* (pp. 94–124). Minneapolis: University of Minnesota.

Schwarcz, H. P. (1986). Geochronology and isotopic geochemistry of speleothems. In P. Fritz, & J. Ch. Fontes, (Eds.), *Handbook of environmental isotope geochemistry* (pp. 271–303). Amsterdam: Elsevier.

Siegenthaler, U., & Oeschger, H. (1980). Correlation of ^{18}O in precipitation with temperature and altitude. *Nature*, *285*, 314–317.

Siegenthaler, U., & Matter, H. A. (1983). Dependence of $\delta^{18}O$ and δD in precipitation on climate. *Palaeoclimates and palaeowaters*: *A collection of environmental isotope studies* (pp. 37–49). Vienna: International Atomic Energy Agency.

Sibley, D. F., & Gregg, J. M. (1987). Classification of dolomite rock textures. *Journal Sedimentary Petrology*, *57*, 967–975.

Starkel, L. (1991). Long-distance correlation of fluvial events in the temperate zone. In L. Starkel, K. J. Gregory, & J. B. Thornes, (Eds.), *Temperate palaeohydrology* (pp 473–495). New York: Wiley.

Stuiver, M., & Reimer, P. J. (1993). Extended ^{14}C data base and revised CALIB 3.0 ^{14}C age program. *Radiocarbon*, *35*, 215–230.

Stuiver, M., Grootes, P. M., & Braziunas, T. F. (1995). The GISP2 $\delta^{18}O$ climate record of the past 16,500 years and the role of sun, ocean and volcanoes. *Quaternary Research*, *44*, 341–354.

Sunagawa, I. (1984). Growth of crystals in nature. In I. Sunagawa (Ed.), *Materials science of the earth's interior* (pp. 63–105). Tokyo: Terra Scientific.

Talma, A. S., & Vogel, J. C. (1992). Late Quaternary paleotemperature derived from a speleothem from Cango Caves, Cape Province, South Africa. *Quaternary Research*, *37*, 203-213.

Taylor, K. C., Hammer, C. U., Alley, R. B., Clausen, H. B., Dahl–Jensen, D., Gour, A. J., Gundestrup, N. S., Kipfstuhl, J., Moore, J. C., & Washington, E. D. (1993). Electrical conductivity measurements from the GISP2 and GRIP Greenland ice cores. *Nature*, *366*, 549–552.

Verrecchia, E. P., & Verrecchia, K. E. (1994). Needle-fiber calcite: a critical review and proposed classification: *Journal of Sedimentary Research*, *A64*, 650–664.

von Grafenstein, U., Erlenkeuser, H., Kleinmann, A., Müller, J., & Trimborn. P. (1994). High-frequency climatic oscillations during the last deglaciation as revealed by oxygen-isotope records of benthic organisms (Amersee, southern Germany). *Journal of Paleolimnology*, *11*, 349–357.

von Grafenstein, U., Erlenkeuser, H., Müller, J., Trimborn, P., & Alefs, J. (1996). A 200 year mid-European air temperature record preserved in lake sediments: An extension of the $\delta^{18}O_p$-air temperature relation into the past. *Geochimica Cosmochimica Acta.*, *21*, 4025–4036.

Wenk, H. R., Barber, D. J., & Reeder, R. J. (1983). Microstructures in carbonates. In: R. J. Reeder (Ed.), *Carbonates*: *Mineralogy and chemistry*, (pp. 301–367). Rev. Mineralogy, Vol. 11.

Ward, W.B., & Reeder, R. J. (1993). The use of growth microfabrics and transmission electron microscopy in understanding replacement processes in carbonates. In R. Rezak, & D. L. Lavoie (Eds.), *Carbonate microfabrics* (pp. 253–264). New York: Springer.

Wright, H. E. Jr. (1992). Patterns of Holocene climate change in the midwestern United States. *Quaternary Research*, *38*, 129–134.

Yu, Z., McAndews, J. H., & Eicher, U. (1997). Middle Holocene dry climate caused by atmospheric circulation patterns: Evidence from lake levels and stable isotopes. *Geology*, *25*, 251–254.